Accelerating Cleanup of the Defense Nuclear Legacy

Quarterly Technical Progress Report
for the period
April 1, 2008 – June 30, 2008

Dr. W. Glenn Steele, Interim Principal Investigator

Report No. 07040R06

Prepared for the U.S. Department of Energy
Agreement No. DE-FC01-06EW-07040

Institute for Clean Energy Technology
Mississippi State University
205 Research Boulevard
Starkville, MS 39759

icet@icet.msstate.edu
www.icet.msstate.edu

Acknowledgement
This material is based upon work supported by the Department of Energy under award number DE-FC01-06EW-07040

Table of Contents

List of Tables

List of Figures

EXECUTIVE SUMMARY

Task 1. Modeling and Experimental Support for High-Level SRS Salt Disposition Alternatives

Saltcake dissolution simulations on the waste contained in SRS tank 25F are reported. The calculations employed the DWPF recycle stream as diluent. The waste was high in sodium nitrate. As the dilution proceeded, the predicted ion concentrations followed either the dissolution and subsequent dilution or simply a dilution profile. Most all of the soluble salts are expected to dissolve at 88% dilution by weight. As the dilution proceeded, the solids speciation went from sodium nitrate to gibbsite dominant. Additional diluent was added past the 88% dilution by weight value; however, a better scenario may be to leach the aluminum remaining in the tank. Sodium aluminosilicate solids were not predicted to form, either within the tank or in the associated transfer streams.

Subsequent blending of some of the transfer stream with the Batch 5 leachate is reported. Here the total solids expected to re-precipitate upon blending were less than 1% by weight. The main advantage in using the leachate stream appears to be in the ability to control the nitrite and hydroxide such that the streams satisfy existing corrosion guidelines. Further calculations using the remaining streams not discussed here will allow for an estimation of the amount of the total volume of leachate required. This, in turn, can then be compared to the total volume of leachate produced in the caustic addition process for Batch 5. Additional simulations and experiments will be necessary to fully evaluate the blending scenario using different saltcake source wastes.

Task 2. Process Improvements for the Defense Waste Processing Facility (DWPF)

Laser induced breakdown spectroscopy (LIBS) is a diagnostic technique that can measure the concentrations of various elements in a test sample. This project evaluates LIBS as an on-line, simultaneous multi-species analysis of the Defense Waste Processing Facility slurry sample. Commonly, LIBS uses laser pulses to ablated and excite sample in one step. In Dual-pulse (DP) LIBS, an ablation pulse is followed by a re-excitation pulse few microsecond apart to ablate and excite sample. Recently, DP LIBS has shown great potential to improve the analytical performance of LIBS. During this work period, we continue the test of the new dual-pulse laser for DP-LIBS measurement. Various experimental configurations and experimental parameters were tested to obtain the optimized experimental condition to operate this DP-LIBS system. An optical box for the DP-LIBS field demonstration was designed and fabricated. This sturdy optical box is designed for easy optical alignment and transportation.

Task 3. High Efficiency Particulate Air

Work continued on establishing standards for HEPA filter use in nuclear and defense facilities. Procedures for performing autopsies on filter media have been established.

Task 4. Support of Hanford Single Shell Tank Waste Disposition

Development of a neural network to augment the chemistry in HTWOS, specifically for the C tank farm retrieval continued. An ESP program process model using the Mobile Retrieval System was used to simulate the retrieval of waste from C-101 into AY-101. Additionally, the use of fresh water versus AY-101 liquid for flushing was compared.

Task 5. Long-Term Monitoring of Selected Heavy Metal and Radionuclide Contaminants and Application of Phytoremediation

During this quarter, we started a study on impact of Mg on toxicological effects from Hg in Indian mustard. The new experiments were designed to investigate mitigation of mercury toxicity using plant nutrition management since Hg causing damages to the photosysthesis system of plants.

Meanwhile, data and sample analyses of previous greenhouse studies on oxidative stress of Indian mustard by Hg were continued. Mercury showed a significant phytotoxicity (in terms of biomass, leaf relative water contents and leaf structure change) in two cultivars of Indian mustard at elevated concentrations ($\geq$2 mg L^{-1}). Chemical analysis showed high accumulation of mercury in plant tissues, especially in roots; this result indicates that Indian mustard might be a potential candidate plant for phytofiltration of contaminated water and phytostabilization of mercury contaminated soils. Further experimental studies were planned to verify these findings.

Task 6. Saltsone

This project is designed to assist the Savannah River Site (SRS) in the production of the Saltstone waste form from low-level tank waste. The expectation of increased aluminum content in the next batch has raised concerns about an excess heat of hydration which may create problems for the storage of the waste form. The facility also relies on vault temperature modeling to protect vault temperature limits. These studies are designed to examine the effects of the heat created by the reactions and to discover methods for either dealing with the excess heat or preventing it from occurring in the first place.

Task 7. Bioavailability studies of mercury and other heavy metal contaminants in ecosystems of selected DOE sites

During this quarter, all experimental work was temporally suspended due to ICET funding cuts. However, we continued in analyzed the previous experiments on oxidation reactions of pure HgS and contaminated Oak Ridge soils with two iron oxides (hematite, Fe_2O_3 and magnetite Fe_3O_4). Magnetite effectively oxidized HgS from both pure HgS system and Oak Ridge contaminated soils with HgS, while hematite released very little SO_4 from both systems.

Task 8. Hanford Tank Inspection

At end of the previous quarter, ICET was informed that because of the downward revision of the ICET Cooperative Agreement CA08 budget, that there are no funds to support the Hanford in-tank characterization effort for the current Cooperative Agreement year. ICET administrators subsequently issued a stop-work order. The bi-weekly conference calls with our Hanford collaborators were suspended. At this time, no further efforts are planned until funding becomes available.

Task 1

Support of SRS Salt Disposition

Jeffrey S. Lindner and Laura T. Smith

INTRODUCTION

Major needs in the SRS tank farms are dictated by the desire to separate actinides and cesium from salt wastes permitting the processing of the high activity waste fraction in the Defense Waste Processing Facility (DWPF) and stabilization of the lower activity waste as saltstone. Towards this end, efforts are currently underway for the development of the Salt Waste Processing Facility (SWPF) containing the Actinide Removal Process (ARP) and Caustic Side Solvent Extraction Unit (CSSX).[1-3] Current progress involves the pilot-scale testing of the CSSX process wherein solids re-precipitation and emulsions formation has been observed within the contactors and in wash and scrub liquors.

In addition the processing of sludge (caustic addition to Batch 5) to reduce the fraction of aluminum routed to the DWPF is scheduled for FY'08. [4-6]. It is expected that aluminum-rich supernatants will be processed in the same manner as salt waste. Here, however, the downstream implications of mixing the aluminum-rich supernatant with DDA fractions from salt waste retrieval and other streams such as the DWPF recycle are unknown. The silicon concentration within the DWPF recycle stream along with the high aluminum loading in the Batch 5 (and potentially other sludge batches) leachate may indicate the formation of intractable aluminosilicates which will create a downstream problem owing to negligible solubility and the propensity for co-precipitation of uranium.

This project is divided into 2 Tasks. Task 1.1 is aimed at evaluation of the CSSX process through experiments and thermodynamic modeling. In collaboration with Parsons Engineering, the analysis of solids and scales observed in various portions of the process, including contactors, filters and solids formed in drain tanks. These solids will be analyzed using x-ray diffraction and inductively coupled plasma emission spectroscopy. Laboratory kinetic experiments are also planned to examine the stability of simulants to be used in pilot-scale testing at Parsons.

Task 1.2 is aimed at assessing stream stability for blended compositions arising from potential tank farm operations. Any stream blending will be performed upstream of the SWPF. The primary streams of concern are the DWPF Recycle stream, which consists of DWPF overheads and is routed to the tank farm, high aluminum concentration streams from sludge leaching operations (50% NaOH) and dissolved salt streams originating from saltcake dissolution. Predicted compositions will be assessed through calculated parameters such as percent solids by weight, aqueous phase density, adherence to

corrosion waste acceptance criteria, [7] and ionic strength. Initial examination of blending along with the results from Task 1.1 allow for a starting point for SWPF waste acceptance criteria. [8]

WORK ACCOMPLISHED

Task 1.1

Work continued on the characterization of samples received from Parsons. XRD diffraction patterns were obtained and ICP OES results are being obtained to determine the solids and the percent of solids found in the samples [9]. Additional work has started on the analysis of an emulsion sample. Initial attempts to separate the emulsion phases have been complicated by the organic constituents in the sample. Other routes are being investigated to separate the organic and aqueous phase and allow characterization of the solids using XRD and ICP OES and organics by GC/MS.

Task 1.2

Saltcake Dissolution of Tank 25F Waste using the DWPF Recycle Stream as Diluent

Blending studies were directed at the saltcake composition from Tank 25F, the use of the DWPF recycle stream as diluent and the addition of the Batch 5 leachate stream. The base composition for the waste in SRS tank 25F was taken from the analysis of core samples performed by Martino et al. [10]. Initial tank farm operations routed approximately 100,000 gallons of supernatant to Tank 41H, Figure-1, followed by the addition of 960,000L (250,000 gal.) of water. Thereafter, around $1.5x10^6$ L (400,000 gal.) of dissolved salt solution was transferred to tank 41H.

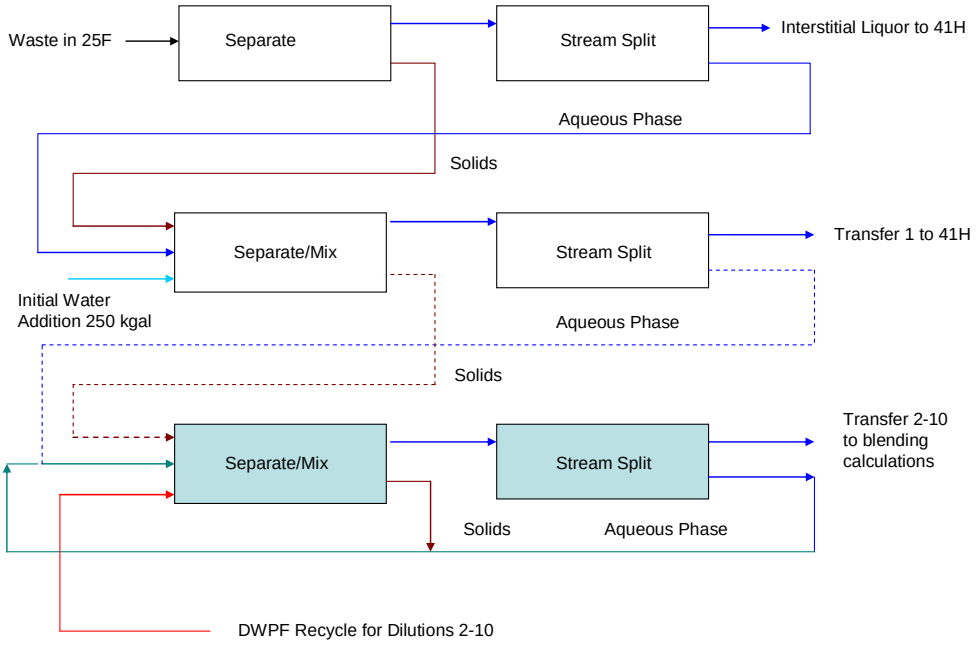

Figure-1 Flowsheet employed for the ESP calculations. The blue lines correspond to the aqueous phase while brown lines denote solids.

Following the transfers to tank 41H, the remaining solids and aqueous phase was mixed with 960,000L of the DWPF recycle stream. The volume of the transfer stream was determined from the solids volume remaining and the solids volume fraction prior to the initial water addition step. Dividing the solids volume by the volume fraction provides the total waste volume that will remain in the tank. Further subtracting the solids volume from this total volume and then dividing the aqueous phase volume that will remain in the tank by the total aqueous volume following the addition of diluent, allows for determining the split fractions for the aqueous phase.

The ESP chemistry model, using the MSU ICET double salt along with the OLI Systems Inc. Corrosion and Public databases, accounted for all of the constituents in the Tank 25F waste along with the compositions for the DWPF recycle stream and the aqueous phase leachate from DWPF batch 5 feed. Information on the Batch 5 leachate and the DWPF recycle stream were presented in the previous quarterly report [9]. A number of different process flowsheets were used to enable the overall calculations. Separate processes were developed for the leaching of batch 5, the preparation of the DWPF recycle stream, the 25F waste dissolution, and finally, blending the transfer streams with the leachate. The calculations, especially those based on Figure-1 should be considered as examples. Specifically, the flowsheet of Figure-1 adds 960,000 L of the recycle stream at each stage of the dissolution. In all likelihood, SRS tank farm operations may not allow for a constant volume addition of diluent owing to receiving tank waste space limitations or the ability to process the waste directly through the salt waste processing facility (SWPF). The results given below, however, allow for an examination of the dissolution of the waste in 25F and an initial assessment of the ability to blend resulting supernatants with the high hydroxide, high aluminum leachate stream.

Stream parameters for the waste composition prior to each dissolution stage are given in Table-1. The results are for the aqueous and solid phases in the tank prior to dilution. The near-constant volume fractions for the aqueous and solid phases respectively, V1 and V2, indicate that the transfer streams have been properly accounted for in the stream split operations block of Figure-1. The dissolution process can be either accounted for in the stage number of by percent dilution by weight. The later value was calculated using the mass of the waste in 25F immediately prior to the first water addition (after the initial transfer of supernatant to tank 41H). The calculations range from the base waste at 0% to ~110% dilution by weight. The principal solid in tank 25F was sodium nitrate, Table-2. Other soluble salts at much lesser amounts included sodium carbonate monohydrate ($Na_2CO_3 \cdot H_2O$), the double salts Na_3FSO4, $Na_6(SO_4)_2CO_3$, and natrophosphate ($Na_7F(PO_4)_2 \cdot 19H_2O$), and sodium oxalate ($Na_2C_2O_4$). Following the dilution of stage 7, ~76% dilution by weight, all of the soluble salts with the exception of sodium oxalate and natrophosphate have dissolved. The solid $Ca_5(PO_4)_3F$ (fluoroapetite) tends to form as dilution proceeds. The chromium and iron solids were predicted to remain constant throughout the simulation. As the dilution proceeds, re-precipitation of $Pu(OH)_4$ and UO_2

is expected. The model predicts the formation of $Pu(OH)_4$ at stage 4; however, these loadings are subsequently on the order of 4 to 25g. Similar comments apply to UO_2 where the loadings range from 7 to 51g.

Table-1 Waste compositions in 25F at each stage of the flowsheet following the splitting of each transfer stream...

Stage	1	2	3	4	5	6	7	8	9	10
% dilution by wt	0.00	11.91	24.65	37.39	50.13	62.86	75.60	88.34	101.08	113.81
Aqueous										
H_2O	1.06E+06	9.00E+05	7.11E+05	5.85E+05	4.32E+05	2.85E+05	1.40E+05	4.92E+04	5.57E+04	5.36E+04
Mass (kg)	1.99E+06	1.70E+06	1.36E+06	1.13E+06	8.42E+05	5.57E+05	2.75E+05	8.31E+04	6.20E+04	5.79E+04
Volume (L)	1.44E+06	1.23E+06	9.78E+05	8.16E+05	6.09E+05	4.03E+05	1.99E+05	6.33E+04	5.76E+04	5.48E+04
Density (g/L)	1381.62	1384.17	1389.78	1385.08	1383.23	1382.64	1381.82	1312.72	1075.65	1056.58
pH	15.12	14.73	14.48	14.19	14.01	13.91	13.88	13.65	13.43	13.44
Ionic Strength	12.43	12.06	12.17	11.80	11.68	11.64	11.53	8.29	1.98	1.53
Solids										
Mass (kg)	5.92E+06	5.04E+06	4.19E+06	3.35E+06	2.51E+06	1.66E+06	8.25E+05	2.76E+05	2.55E+05	2.43E+05
Volume (L)	2.60E+06	2.21E+06	1.83E+06	1.47E+06	1.10E+06	7.26E+05	3.57E+05	1.14E+05	1.04E+05	9.87E+04
Density (g/L)	2278.55	2280.96	2283.58	2284.97	2286.01	2287.65	2311.50	2419.33	2458.55	2463.23
Total Stream										
Mass (kg)	7.90E+06	6.74E+06	5.54E+06	4.48E+06	3.35E+06	2.22E+06	1.10E+06	3.59E+05	3.17E+05	3.01E+05
Volume (L)	4.04E+06	3.44E+06	2.81E+06	2.28E+06	1.70E+06	1.13E+06	5.55E+05	1.77E+05	1.61E+05	1.53E+05
Density (g/L)	1958.78	1960.74	1972.63	1963.08	1963.68	1964.58	1978.97	2024.10	1964.67	1960.87
% solids by wt	74.85	74.79	75.49	74.76	74.85	74.88	75.02	76.84	80.45	80.76
% water by wt	13.41	13.36	12.82	13.05	12.90	12.84	12.78	13.73	17.58	17.81
V1	0.36	0.36	0.35	0.36	0.36	0.36	0.36	0.36	0.36	0.36
V2	0.64	0.64	0.65	0.64	0.64	0.64	0.64	0.64	0.64	0.64

Table-2 Solids mass (kg) in tank 25F at each stage of the dissolution following the splitting of each transfer stream.

Stage	1	2	3	4	5	6	7	8	9	10
% dilution by wt	0.00	11.91	24.65	37.39	50.13	62.86	75.60	88.34	101.08	113.81
$Al(OH)_3$	2.62E+05	2.72E+05	2.64E+05	2.61E+05	2.56E+05	2.50E+05	2.45E+05	2.42E+05	2.39E+05	2.35E+05
$Ca_5(PO_4)_3F$			6.12E-01	1.28E+00	1.94E+00	2.60E+00	3.29E+00	3.98E+00	4.66E+00	5.34E+00
Cr_2O_3	4.12E+02	4.12E+02	4.12E+02	4.12E+02	4.12E+02	4.12E+02	4.12E+02	4.12E+02	4.12E+02	4.12E+02
Fe_2O_3	3.99E+03	3.99E+03	3.99E+03	3.99E+03	3.99E+03	3.99E+03	3.99E+03	3.99E+03	3.99E+03	3.99E+03
$Na_2C_2O_4$	2.65E+04	2.57E+04	2.47E+04	2.37E+04	2.27E+04	2.16E+04	2.05E+04	1.89E+04	1.19E+04	3.24E+03
$Na_2CO_3 \cdot H_2O$	2.34E+05	1.19E+05	6.99E+03							
Na_3FSO_4	1.33E+04	1.22E+04	1.05E+04	9.44E+03	8.29E+03	7.09E+03	4.34E+03			
$Na_6(SO_4)_2CO_3$	2.84E+05	2.52E+05	2.22E+05	1.61E+05	9.02E+04	1.65E+04				
$Na_7F(PO_4)_2 \cdot 19H_2O$	1.11E+04	1.11E+04	1.11E+04	1.10E+04	1.09E+04	1.07E+04	1.07E+04	1.05E+04		
$NaNO_3$	5.08E+06	4.34E+06	3.64E+06	2.88E+06	2.11E+06	1.35E+06	5.40E+05			
$Pu(OH)_4$				4.48E-03	9.15E-03	1.37E-02	1.82E-02	2.26E-02	2.42E-02	2.55E-02
UO_2								7.33E-03	3.21E-02	5.10E-02

A large decrease in the ionic strength, Table-1, was predicted and the percent solids distribution shifted from $NaNO_3$ as the major solid to gibbsite, $Al(OH)_3$, Figure-2. Dissolution of the other soluble salts is given in Figure-3. The first solid predicted to completely dissolve was sodium carbonate monohydrate. This was followed by the dissolution of the carbonate containing double salt and then sodium nitrate. Once the ionic strength decreases after stage 7 the overall percentages of the remaining salts is increased. At this point continued dissolution of these salts can proceed.

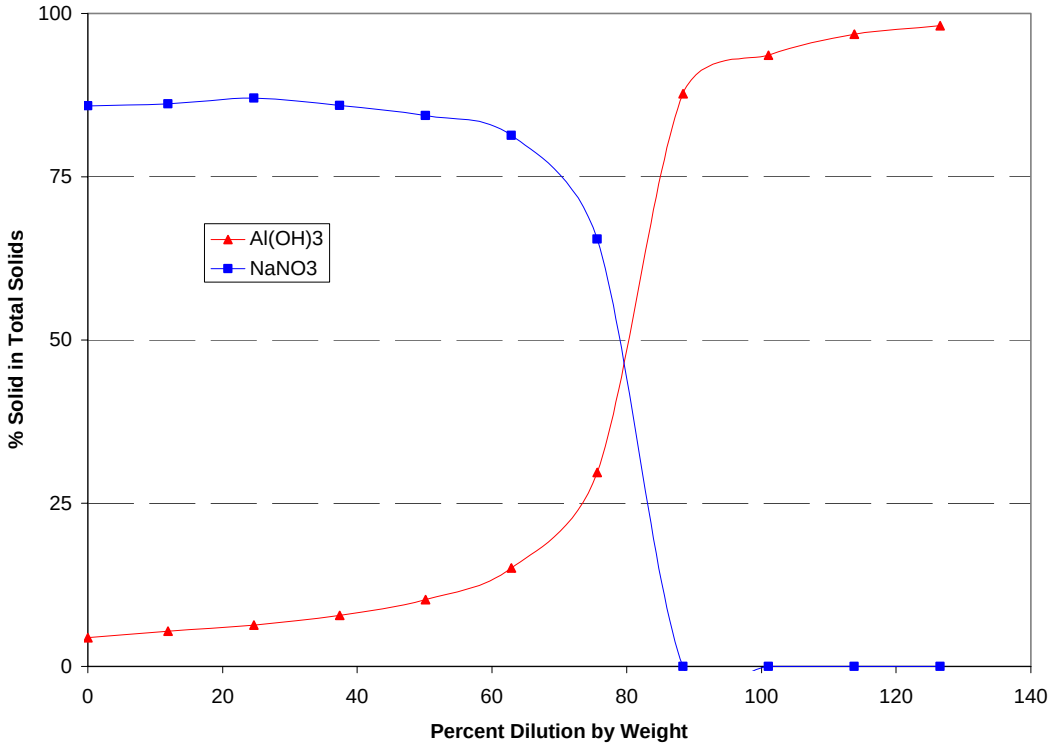

Figure-2 Percent of sodium nitrate and gibbsite as a function of percent dilution by weight.

The shift from a nitrate to an aluminum dominated solids mix might best be handled by not continuing to add diluent. Dissolution of the gibbsite using water is not favorable and following stage 7 other options, such as caustic leaching may be effective. These simulations have not yet been performed but are planned.

The corollary to the solids dissolution is the concentration of major anions and cations at the different dilution stages, Figure-4. Sodium ion loadings are somewhat constant until the dissolution of $NaNO_3$ is complete. The curves for both the nitrate and carbonate anions represent solids dissolution corresponding to an increase in ion concentrations followed by a decrease in concentration as the stream are diluted. The hydroxide loading is predicted to initially be around 3M and upon the addition of the DWPF recycle stream decays as dilution is occurring. This decrease has implications on corrosion control. Specifically for nitrate concentrations between 5.5 and 8.5M, the sum of the hydroxide

and nitrite concentrations should be greater than 1.1M [7]. The simulations predict that transfer streams 1, 2, and 3 are within the corrosion guidelines. All of the other streams are outside of the acceptable corrosion range and must be augmented with hydroxide and/or nitrite.

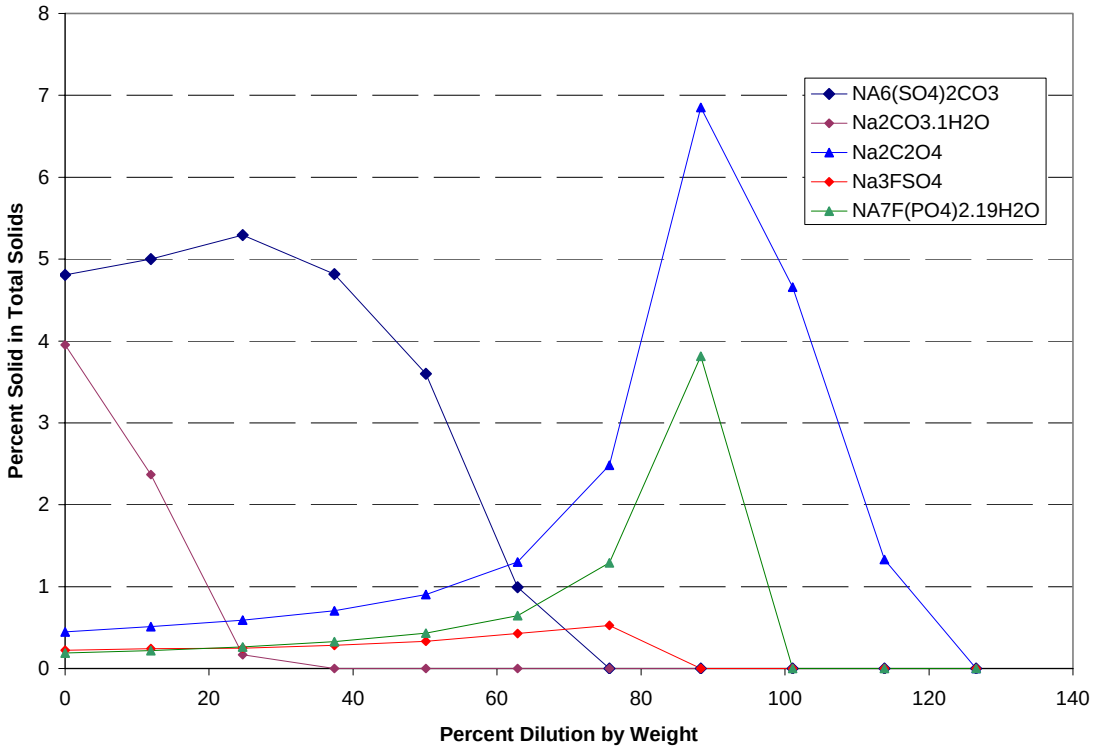

Figure-3 Percent minor solids in total solids as a function of dilution stage.

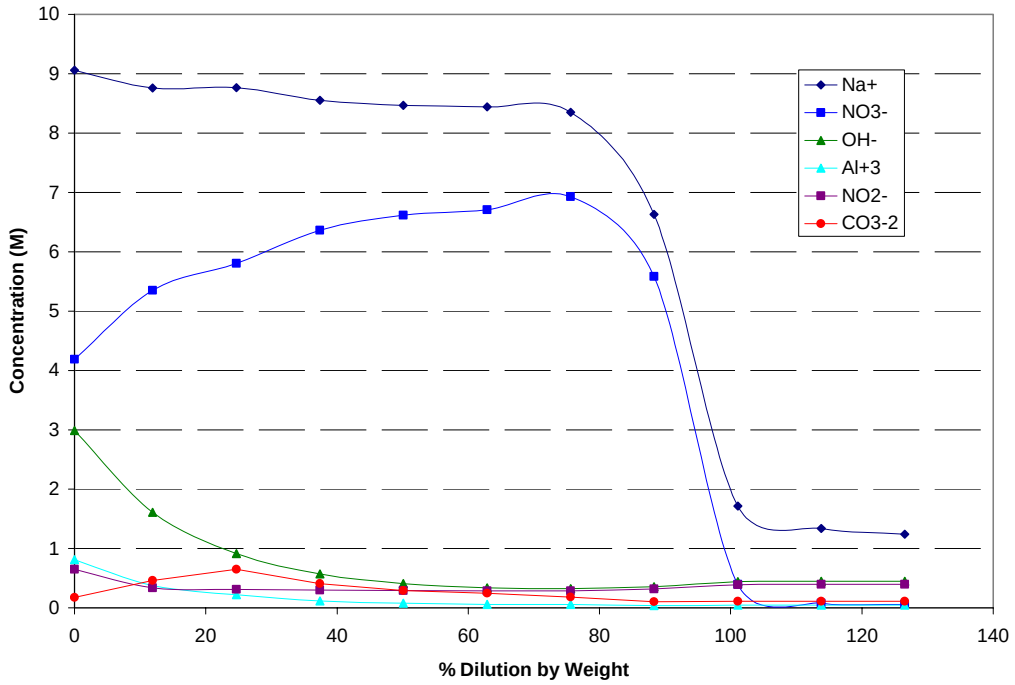

.

Figure-4 Supernatant ion concentrations as a function of dissolution of the waste in SRS tank 25F using the DWPF recycle stream as a diluent.

Physical parameters and ion concentrations for the transfer streams are given in Table-3. All results correspond to a temperature of 30°C. As the dilution proceeds, the pH and ionic strength slowly decrease. The density is constant until around stage 7 where a large portion of the nitrate has dissolved. Upon complete dissolution of $NaNO_3$ the ionic strength and density decrease significantly, the nitrate has dissolved. The concentrations of ions in the waste supernatant are the same as for the transfer streams at the different dilution stages The table contains data for most ions with the exception of sludge constituents, Fe^{+3}, Ca^{+2} Hg^{+2}, etc. Ions that were at loadings less than $1x10^{-9}$M are omitted. Analysis of the concentrations according to corrosion specifications indicated that transfer streams 1 and 2 are in compliance. None of the other streams were within specifications; however, the blending simulations described below indicate that these streams can be stabilized with small volume additions of the Batch 5 leachate.

Of some concern in using the DWPF recycle stream is the presence of silicon, which under some conditions, has a tendency to form insoluble and generally intractable cancrinites (sodium aluminosilicates, NAS). The results in Table-3 indicate that the silicon loading stays below $5x10^{-4}$M. The lack of any NAS solids predicted in these simulations reflects the low concentration of Si in the supernatant; however, NAS formation cannot definitely be ruled out owing to the databases employed for the calculations. Earlier work at SRNL produced the zeolite database, which accounted for important materials such as sodalite and cancrinites [11]. The database was compatible with ESP versions 6.3 and 6.5; unfortunately, the ESP version currently in use is version

Table-3 Physical properties and ion concentrations (M) of the transfer streams.

Stage	0	1	2	3	4	5	6	7	8	9	10
% dilution by wt	0	11.91	24.65	37.39	50.13	62.86	75.60	88.34	101.08	113.81	126.55
Total (kg)	1.99E+06	2.11E+06	2.20E+06	2.07E+06	2.14E+06	2.14E+06	2.36E+06	1.75E+06	1.05E+06	1.02E+06	1.02E+06
Volume (L)	1.44E+06	1.52E+06	1.58E+06	1.50E+06	1.55E+06	1.54E+06	1.61E+06	1.33E+06	9.75E+05	9.68E+05	9.66E+05
Density (g/L)	1381.62	1384.17	1389.78	1385.08	1383.23	1382.64	1381.82	1312.72	1075.65	1056.58	1050.77
pH	15.12	14.73	14.48	14.19	14.01	13.91	13.88	13.65	13.43	13.44	13.44
Ionic Strength	12.43	12.06	12.17	11.80	11.68	11.64	11.53	8.29	1.98	1.53	1.38
Na^{+}	9.06	8.76	8.77	8.55	8.47	8.44	8.35	6.63	1.71	1.34	1.24
NO_3^{-}	4.19	5.35	5.80	6.37	6.61	6.70	6.93	5.58	0.40	0.08	0.06
OH^{-}	2.99	1.61	0.92	0.57	0.41	0.34	0.32	0.35	0.44	0.45	0.45
Al^{+3}	0.81	0.38	0.22	0.11	0.08	0.06	0.06	0.04	0.04	0.05	0.05
NO_2^{-}	0.65	0.34	0.31	0.30	0.29	0.29	0.29	0.32	0.39	0.40	0.40
CO_3^{-2}	0.18	0.46	0.65	0.41	0.29	0.24	0.18	0.10	0.11	0.11	0.11
SO_4^{-2}	4.71E-02	8.75E-02	1.06E-01	1.81E-01	2.41E-01	2.73E-01	1.81E-01	4.29E-02	2.84E-03	3.71E-04	2.32E-04
F^{-}	1.44E-02	9.68E-03	8.36E-03	6.01E-03	5.28E-03	5.12E-03	8.01E-03	1.82E-02	1.55E-02	9.26E-04	1.05E-04
Si^{+4}	0.00E+00	0.00E+00	1.84E-04	2.82E-04	3.26E-04	3.44E-04	3.48E-04	3.88E-04	4.81E-04	4.88E-04	4.89E-04
$C_2O_4^{-2}$	1.05E-03	2.70E-03	4.14E-03	5.07E-03	5.51E-03	5.70E-03	6.01E-03	9.37E-03	5.13E-02	6.59E-02	2.73E-02
PO_4^{-3}	2.73E-05	3.14E-05	5.21E-05	0.000115	0.000193	0.000251	0.000225	0.000314	0.028603	0.001607	8.39E-05
K^{+}	0.053564	0.028015	0.013425	0.005678	0.002151	0.000672	0.000361	5.14E-05	3.15E-06	1.77E-07	9.54E-09
Cl^{-}	0.011483	0.006006	0.002878	0.001217	0.000461	0.000144	7.73E-05	1.1E-05	6.75E-07	3.8E-08	2.05E-09
U^{+4}	0.00E+00	0.00E+00	4.28E-07	6.55E-07	7.57E-07	7.99E-07	8.09E-07	8.82E-07	1.03E-06	1.06E-06	1.05E-06
Tc^{+4}	0.00E+00	0.00E+00	3.57E-07	5.46E-07	6.31E-07	6.66E-07	6.74E-07	7.51E-07	9.30E-07	9.45E-07	9.47E-07
Cs^{+}	2.96E-07	1.55E-07	1.75E-07	1.85E-07	1.90E-07	1.91E-07	1.92E-07	2.12E-07	2.62E-07	2.67E-07	2.67E-07
Am^{+3}	0.00E+00	0.00E+00	5.21E-08	7.97E-08	9.21E-08	9.73E-08	9.85E-08	1.10E-07	1.36E-07	1.38E-07	1.38E-07
Pu^{+4}	0.00E+00	0.00E+00	6.06E-09	3.06E-09	1.41E-09	9.43E-10	8.20E-10	1.22E-09	1.00E-08	1.18E-08	1.21E-08

8.0. The zeolite database is no longer compatible with the ESP software owing to improvements in the model and in the default Public database. In an attempt to remedy this situation, the corrosion database was employed here.

There are three NAS species in the corrosion database, low and high albite ($NaAlSi_3O_8$) and natrolite ($Na_2Al_2Si_3O_{10}\cdot 2H_2O$). Predicted values for the scaling tendencies for these molecules were $1x10^{-10}$, $5x10^{-12}$, and $2x10^{-4}$. These values are far away from a value of unity where solids formation is expected. Although NAS formation cannot be ruled out it appears, based on these simulations, that NAS will not form either in the tank or in the transfer stream. Further calculations and experiments will be needed to clarify this point with different source tank compositions and in the subsequent blending of streams prior to routing to the salt waste processing facility (SWPF).

Dissolution of the saltcake in Tank 25F using the DWPF recycle appears straightforward. The process will produce some compositions that are outside corrosion specification and these streams will require blending with other streams containing higher hydroxide and/or nitrite loadings. The second part of the initial blending simulations is described below. Here the transfer streams from the dissolution of the waste in 25F are mixed with various volumes of the leachate from caustic treatment of DWPF batch 5.

Mixing of 25F Transfer streams with the Batch 5 Leachate

Results for the Batch 5 leachate were presented previously [9]. The main properties of the stream are given in Table-4. The major properties of the composition are the low density and ionic strength, the moderate pH and the high aluminum (~0.77M) and high "free" hydroxide (~3.6M).

Table-4 Properties of the Batch 5 Leachate.

Density (g/L)	1037.00
pH	12.33
Ionic Strength	1.10
Na^+	5.09
NO_2^-	0.36
NO_3^-	0.23
"free" OH^-	3.62
total OH^-	6.70
Al^{+3}	0.77
Cl^-	4.95E-03
SO_4^{-2}	1.83E-02
F^-	1.57E-03
CO_3^{-2}	2.82E-02
$C_2O_4^{-2}$	3.58E-03
PO_4^{-3}	6.22E-04
K^+	2.13E-03

Initial leachate additions were set at 10, 20, 40 60, and 80% by volume. Results, for all streams, indicated that corrosion specifications were satisfied at the 20% by volume addition. Thus, some additional simulations were performed at 14 and 17% Batch 5 leachate added. The final temperature was set to 23°C. The ESP chemistry model was the same as that for the saltcake dissolution calculations above.

The main parameters of interest included the percent solids by weight, the percent water by weight, the resulting density, pH, ionic strength, and principal ion concentrations. As noted above the concentration of nitrate anion dictates the corrosion requirements. Efforts were made to establish correlations among the parameters. If the solids loading remained less than about 1% by weight, the main goal of the simulations was to assess the use of the leachate stream for corrosion control.

Table 5 contains the results for the addition of the Batch 5 leachate to the transfer stream obtained at stage 3 of the saltcake dissolution process. Cooling transfer stream 3 to 23°C resulted in the re-precipitation of gibbsite and $NaNO_3$. The addition of Batch 5 leachate resulted in dissolution of sodium nitrate. From a process perspective, it is probably best to control the temperature of the transfer stream, if possible, such that solids will not form. The results given here are strictly based upon equilibrium thermodynamics and the dissolution kinetics for gibbsite are known to be slow [12].

$Ca_5(PO_4)_3F$, Fe_2O_3 and $Mg(OH)_2$ are predicted to form upon addition of the leachate. Gibbsite also forms and increases as the volume of leachate added increases. Nonetheless, the overall solids loading as denoted in the percent solids by weight number is quite small. In this case the amount of leachate that should be added will relate to achieving a corrosion compliant composition.

Table 5 Addition of the Batch 5 leachate to transfer stream number 3.

% Leachate addition (by vol.)	tfer 3	tfer 3	10	14	17	20
Temperature (^{o}C)	30	23	23	23	23	23
H_2O (kg)	1.07E+06	1.07E+06	1.21E+06	1.26E+06	1.30E+06	1.34E+06
Total (kg)	2.07E+06	2.01E+06	2.24E+06	2.31E+06	2.37E+06	2.42E+06
Volume (L)	1.50E+06	1.46E+06	1.63E+06	1.69E+06	1.73E+06	1.77E+06
Density (g/L)	1385.08	1380.07	1376.34	1370.92	1366.98	1363.18
pH	14.19	14.40	14.57	14.59	14.61	14.62
Ionic Strength	11.80	11.12	11.01	10.76	10.58	10.41
Na^{+}	8.55	8.31	8.29	8.18	8.11	8.03
NO_3^{-}	6.37	6.07	5.86	5.67	5.54	5.41
OH^{-}	0.57	0.62	0.89	0.86	0.97	1.14
Al^{+3}	0.11	0.08	0.12	0.13	0.13	0.14
NO_2^{-}	0.30	0.31	0.31	0.31	0.31	0.31
CO_3^{-2}	0.41	0.42	0.38	0.37	0.36	0.35
SO_4^{-2}	0.18	0.19	0.17	0.16	0.16	0.16
F^{-}	6.01E-03	6.13E-03	5.59E-03	5.45E-03	5.34E-03	5.25E-03
Si^{+4}	2.82E-04	2.90E-04	2.59E-04	2.50E-04	2.44E-04	2.38E-04
$C_2O_4^{-2}$	5.07E-03	4.89E-03	4.14E-03	4.00E-03	3.90E-03	3.81E-03
PO_4^{-3}	1.15E-04	4.19E-05	2.79E-05	2.59E-05	2.50E-05	2.46E-05
K^{+}	5.68E-03	5.83E-03	5.41E-03	5.31E-03	5.23E-03	5.16E-03
Cl^{-}	1.22E-03	1.25E-03	1.59E-03	1.72E-03	1.81E-03	1.89E-03
U^{+4}	6.55E-07	6.73E-07	6.01E-07	5.81E-07	5.66E-07	5.52E-07
Tc^{+4}	5.46E-07	5.61E-07	5.01E-07	4.84E-07	4.72E-07	4.60E-07
Cs^{+}	1.85E-07	1.90E-07	1.70E-07	1.64E-07	1.60E-07	1.56E-07
Am^{+3}	7.97E-08	8.19E-08	7.32E-08	7.07E-08	6.89E-08	6.72E-08
Pu^{+4}	3.06E-09	3.14E-09	2.81E-09	2.71E-09	2.64E-09	2.58E-09
Solid Phase						
$Al(OH)_3$	1.30E-02	3.80E+03	5.25E+03	6.38E+03	7.23E+03	8.07E+03
$Ca_5(PO_4)_3F$		2.06E-02	7.21E-02	9.30E-02	1.09E-01	1.24E-01
Fe_2O_3		7.58E-03	1.09E-02	1.28E-02	1.42E-02	1.57E-02
$Mg(OH)_2$		4.56E-05	8.50E-05	8.93E-05	9.16E-05	9.34E-05
$Na_2C_2O_4$		6.09E+01	1.62E+02	1.83E+02	1.98E+02	2.12E+02
$Na_7F(PO_4)_2{\cdot}19H_2O$		3.93E+01	7.90E+01	9.34E+01	1.04E+02	1.14E+02
$NaNO_3$		5.84E+04				
Total (kg)	1.30E-02	6.23E+04	5.49E+03	6.65E+03	7.53E+03	8.40E+03
Volume (L)	5.32E-03	2.75E+04	2.27E+03	2.74E+03	3.10E+03	3.46E+03
Density (g/L)	2440.66	2267.01	2424.37	2424.90	2425.25	2425.56
Total Stream						
Total (kg)	2.07E+06	2.07E+06	2.25E+06	2.32E+06	2.37E+06	2.43E+06
Volume (L)	1.50E+06	1.48E+06	1.63E+06	1.69E+06	1.73E+06	1.78E+06
Density (g/L)	1385.08	1396.49	1377.79	1372.62	1368.88	1365.25
% solids by weight	6.27E-07	3.01	0.24	0.29	0.32	0.35
% water by weight	51.71	51.71	53.70	54.41	54.92	55.40

For nitrate anion loadings between 5.5 and 8.5M, the hydroxide concentration should be greater than or equal to 0.6M and the sum of the hydroxide and nitrate concentrations should be greater than or equal to 1.1 [7]. Table 6 provides the results for analysis of the corrosion limits. Only a small amount of leachate, somewhere between 5 and 7%, would result in a summed concentration of nitrite and hydroxide of 1.1M, Figure 5.

Table 6 Corrosion compliance calculations for transfer stream 3 with added Batch 5 leachate. All concentrations are in mol/L.

% Leachate addition (by volume)		tfer 3	tfer 3	10	14	17
Temperature (^{o}C)		30	23	23	23	23
$[NO_3^{-}]$		6.37	6.07	5.86	5.67	5.54
$[OH^{-}]$		0.57	0.62	0.89	0.86	0.97
$[NO_2^{-}]$		0.30	0.31	0.31	0.31	0.31
5.5- 8.5		yes	yes	yes	yes	yes
$[OH^{-}]$	0.6	no	yes	yes	yes	yes
[NO2-] + $[OH^{-}]$	1.1	0.87	0.93	1.20	1.17	1.28
compliant		no	no	yes	yes	yes

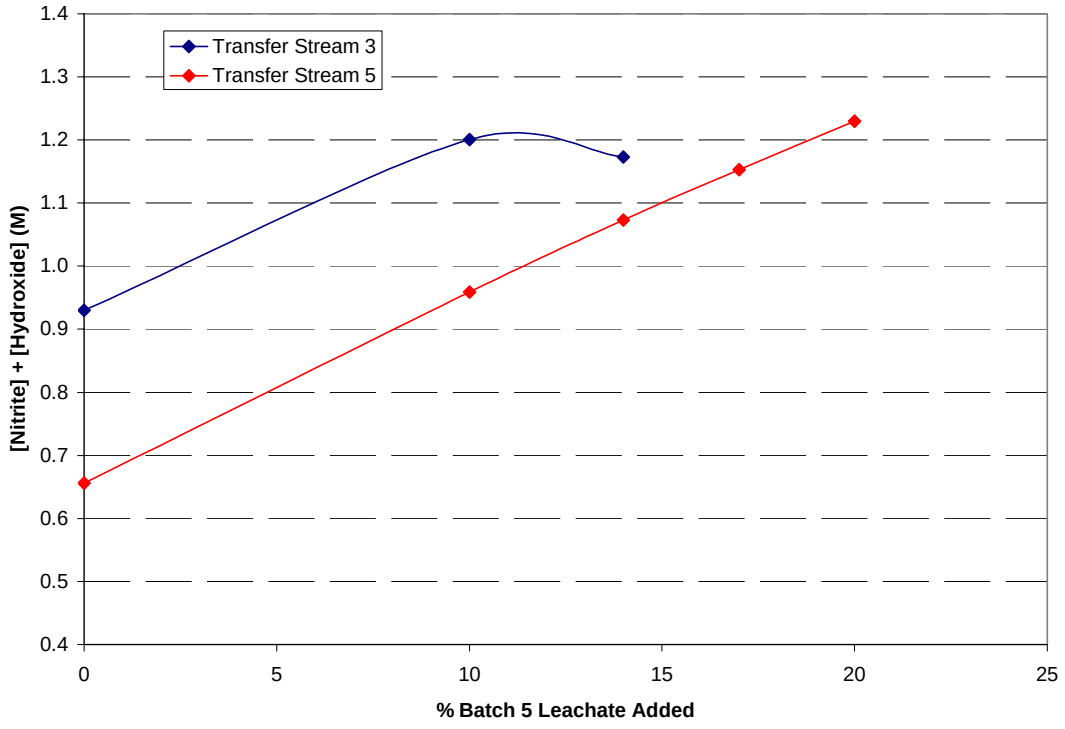

Figure-5 The sum of the nitrite and hydroxide concentration as a function of added Batch 5 leachate.

Addition calculations are in progress for the remaining transfer streams. A second example is also given in Figure 5 where transfer stream 5 is evaluated. In this case, the nitrate anion

concentration was always greater than 5.5. The initial hydroxide concentration was predicted to be 0.34M (Table 3). In order to attain the corrosion specifications around 15% of leachate or 231,000L would be needed. It is expected that as the transfer stream becomes more dilute, toward the end of the dissolution process, the amount of leachate needed to satisfy the corrosion limits would increase.

These initial predictions indicate that the Batch 5 leachate stream can be blended with dissolved salt solutions contained in tank 25F. Additional laboratory and modeling work on other compositions is needed to further verify this result

WORK FORECAST

Efforts are continuing on the characterization of CSSX scale, deposition, and emulsion samples sent by Parson. The primary work in the next quarter will be analysis of the emulsion sample and completion of the XRD and ICP-OES analysis of the solids. A preliminary Letter report has been routed to Parsons and the addition efforts are designed to effect completion of that report. Further saltcake dissolution simulations are planned for another waste composition. Additional calculat6ions assessing options for mobilizing the remaining composition in tank 25 using either a leachate stream or direct caustic addition will be performed.

CONCLUSIONS

The dissolution of the waste contained in SRS tank 25F using the DWPF recycle stream followed previous patterns with regard to SRS tank 41H. The primary differences are the initial waste compositions. The waste in 25F contains a significantly larger fraction of sodium nitrate than any SRS composition examined previously. Resulting streams destined for other tanks and subsequent blending had high nitrate anion concentrations but low hydroxide and nitrite loadings. Consequently, many of the transfer streams examined here will require additives to enable corrosion control. NAS formation was not predicted in these simulations.

Blending simulations if the dissolved salt streams and the leachate from DWPF Batch 5 pre-treatment were performed to assess a number of stream parameters that may influence downstream processing in the Salt waste processing facility (SWPF). The percent solids by weight following mixing of the streams were always less than 1%. The main benefits of adding the recycle stream are for corrosion control and for waste stream disposition. Resulting compositions from both the transfer streams alone and the mixed compositions can be compared to emerging waste acceptance criteria for the salt waste processing facility.

REFERENCES

1. Dimenna, R.A.; Elder, H.H.; Foweler, J.R.; Fowler, R.C.; Gregory, M.V.; Hang, T.; Jacobs, R.A.; Paul, R.K.; Pike, J.A.; Rutland, P.L.; Smith, F.G.; Subosits, S.G.; Taylor, G.A.; Campbell, S.G.; Washburn, F.A. “Bases, Assumptions, and Results of the Flowsheet Calculations for the Decision Phase Salt Disposition Alternatives” WSRC-RP-99-00006, Rev. 3, Westinghouse Savannah River Company, Aiken, SC

(2001).
2. Leonard, R.A.; Aase, S.B.; Arafat, H.; Conner, A.C.; Chamberlain, D.B.; Falkenberg, J.R.; Regalbutto, M.C.; Vandergrift, G.F. "Experimental Verification of Caustic-Side Solvent Extraction for Removal of Cesium from Tank Waste" *Sol. Extr. and Ion Exch*. **21(4)**, *2003*, 505.
3. Campbell, S.G.; Geeting, M.W.; Kennell, C.W.; Law, J.D.; Leonard, R.A.; Walker, D.D. "Demonstration of Caustic-Side Solvent Extraction with Savannah River Site High Level Waste" WSRC-TR-2001-00223, Rev.1, Westinghouse Savannah River Company, Aiken, SC (2001).
4. Weber, E.J. "Aluminum Hydroxide Dissolution in Synthetic Sludges" DP-1617, 1982.
5. Hay, M.S.; Pareizs, J.M.; Bannochie, C.J.; Stone, M.E.; Click, D.R.; McCabe, D.J. "Preliminary Data from the 3L Tank 51H Aluminum Dissolution Test" SRNL-CST-2007-0102, Savannah River National Lab, Aiken, SC (2007)
6. Ketusky, E., "High Level Waste System Impacts from Acid Dissolution of Sludge" CBU-PIT-2005-00260R1, Westinghouse Savannah River Company, Aiken, SC (2005).
7. Fox, L., "CSTF Corrosion Control Program," WSRC-TR2002-00327, Rev. 3, Westinghouse Savannah River Company, Aiken, SC (2003).
8. Waste Acceptance Criteria for Aqueous Waste sent to the Z-Area Saltstone Production Facility (U). X-SD-Z-00001, Rev. 2, 2004.
9.. Lindner, J. S. and L. T. Smith, "Modeling and Experimental Support for High Level SRS Salt Disposition Alternatives," in Accelerating Cleanup of the Defense Nuclear Legacy, Report No.07040R01, Institute for Clean Energy Technology, Mississippi State University, 2008, pg 7.
10. Martino, C. J., et al., "Analysis and dissolution testing of tank 25F core samples (FTF 504513)," WSRC-STI-2007-00123, Rev.0, Savannah River National Laboratory, Aiken, SC, (2007).
11. Choi, A, personal communication (April 14, 2004).
12. Ganor, J., et al., "Kinetics of gibbsite dissolution under low ionic strength Conditions," Geochemica et Cosmochemica Acta, 63,1635, (1999).

Task 2

Process Improvements for the Defense Processing Facility (DWPF)

Jagdish P. Singh

INTRODUCTION

An near real-time, direct analysis of Defense Waste Processing Facility **(**DWPF) samples will significantly increase analytical throughput and will reduce waste generation in radiological analytical facilities. The goal of this Task is to develop system for rapid analysis of DWPF samples to accelerate waste processing using laser-induced breakdown spectroscopy (LIBS).
The first subtask of this project will provide a system for direct analysis of slurry in the DWPF's analytical shielded cells. The capability of direct analysis of slurry will significantly increase analytical throughput and will reduce waste generation in radiological analytical facilities, providing analyses suitable for waste acceptance and production records. The second subtask is to provide compositional data for plutonium residue feeds before being processed into glass.
LIBS uses a high pulse energy laser beams to produces a micro plasma to vaporize, dissociate, excite, or ionize species on material surfaces. The study of the atomic emission from the micro plasma provides information about the composition of the material. LIBS is a powerful analytical tool which is suitable for quick and on-line elemental analysis of any phase of material.[1-3] The laser light and emitted signal can be delivered via optical fiber so it is useful for hazardous situations. LIBS can provide an accuracy of 3-5% for elements with concentration >1% and an accuracy of 5-10% or better for minor elements in solid samples.

WORK PERFORMED

LIBS can provide real-time elemental analysis with all sample types with little or no preparation. However, the limit of detection of LIBS is higher than other laboratory analytical techniques. Recent year, the development of Double-Pulse (DP) LIBS technique grow rapidly. It has shown significant improvement on LIBS detection limit as compared to the single pulse LIBS.[1,2] Dual-pulse LIBS using an ablation pulse followed by a re-excitation pulse to enhance LIBS signal. Few commonly used beam geometries for dual-pulse LIBS are shown in Figure 1.[4,5] Collinear configuration is the easiest aligned DP configuration wherein both pulses are focused on the same point on the sample. In orthogonal reheating configuration, an air spark is formed after ablation. An air plasma is formed above the sample surface prior to ablation in orthogonal pre-ablation spark configuration, The dual pulse crossed beam mode has both laser beam with

certain angle with the sample surface and cross at the same point on the sample. The DP configuration as well as the combinations of laser pulses with different laser wavelengths, energies, and durations were all being studied for LIBS signal enhancement.

The current ICET dual-pulse laser system consists two collinear spatially overlapped lasers. The two laser beam can fire at the desired interpulse delay (generally few to tens microseconds) to ablate and excite sample. Due to the design of this laser system, we will be limit to collinear DP configuration. The effect of interpulse delay time will play a very important role on LIBS enhancements and was investigated in this work period. Our DP experimental setup (as shown in Figure 2) consists of Big Sky Laser (CFR PIV-200) to deliver spatially overlapped collinear beam at 532 nm with 10 Hz frequency. The beam was further projected on a harmonic separator to reflect 532 nm at 90 degree and the transmitted beam was blocked using beam dump. The reflected beam was guided on Al sample using Dichroic mirror and a 10 cm lens to produce breakdown. The LIBS signal was collected in backward direction using a 10 cm leans and using fiber optics. Optical fiber guided the signal to spectrograph with ICCD detector. Initially, the two laser system was external trigger separately with a pulse generator (DG 535, Stanford Research System) to achieve the desired inter pulse delay between the two lasers. However, we found the laser jitter make the inter-pulse delay vary with time. To minimize the fluctuation in interpulse delay, we externally trigger Q-switch by applying appropriate delay on both lasers (as shown in Figure 3). This triggering circuit significantly reduced the fluctuation in the laser output and a more stable interpulse delay can be achieved.

To obtain the characteristic of our DP-LIBS system we study Mg spectral lines using a standard Al alloy as sample. The selection of Mg spectral lines for characteristic study is because signal enhancement of Mg lines at various gate delays by means of the DP-LIBS technique has been reported from both the experimental and theoretical point of view. The study of Mg lines will be used to evaluate the performance of our DP-LIBS system as compared with the signal enhancement reported in literatures. The spectra were collected with 5 accumulations for each one and 10 spectrums were collected for each set. Typical laser energy during the experiment was 80 mJ per pulse. A typical signal enhancement in double pulse LIBS (i.e. $I_{\text{dual pulse}}/I_{\text{single pulse}}$) from Mg lines at 382.935 nm, 383.230 nm and 383.829 m is shown in Figure 4. The data were obtained by using detector gate delay of 15 μs and gate width of 5 μs. The study of the enhancement in Mg lines at various gate delay shows that the maximum enhancement was obtained for higher gate delays (see Figure 5). However LIBS signal decays with time so generally the signal to noise ratio is better for detector gate delay between 1-10μs. The optimum interpulse delay and detector gate delay are matrix dependent. Therefore, it is necessary to experimentally determine the optimum interpulse delay and detector gate delay for different sample matrix. The effect of pulse energy on DP-LIBS signal was also investigated. Data were recorded with different pulse energy ratio between the two laser pulses. We found that using our current experimental configuration the equal laser energy from the two pulses give best signal to noise ratio. A optical box (see Figure 6) for the DP-LIBS system has been designed and fabricated for field demonstration during this work period. The main components in the optical box are two laser heads, beam combiner module, and various optics to focus the laser beam on sample and collect LIBS signal to optical fiber. The optical box has reserved space for easy modification for different applications.

WORK FORECAST

Work will continue on DP-LIBS measurement with solid sample using a compact broadband spectrometer as detection system. The work to direct sampling slurry sample will continue. LIBS data of slurry with various amount of chemical added will be recorded to obtain calibration data for slurry.

CONCLUSIONS

DP-LIBS is a promising technique for improving the elemental analysis performance of LIBS for solid and liquid samples. In this work period a field DP-LIBS system was developed. Testing this field ready DP-LIBS system is in progress. In the initial DP-LIBS test, we use a Czerny-Turner detection system to study the specified species to understand the characteristic of our system and determine the best operation condition. We will later test this system with a new compact broadband spectrometer using pellet and slurry samples.

REFERENCES

1. J. P. Singh and S. N. Thakur, Laser- Induced Breakdown Spectroscopy, Elesvier Science V., Amsterdam, The Netherlands, 2007.
2. A. Miziolek, V. Palleschi and I. Schechter, Laser- Induced Breakdown Spectroscopy (LIBS): Fundamentals and Applications, Cambridge University Press, 2006.
3. Fang-Yu Yueh, Jagdish P. Singh and Hansheng Zhang, “Laser-induced breakdown spectroscopy-elemental analysis”, in *Encyclopedia of Analytical Chemistry,* R.A.Meyers, ed. (Wiley, New York, 2000).
4. V. I. Babushok, F. C. DeLucia Jr., J. L. Gottfried, C. A. Munson, and A. W. Miziolek, "Double pulse laser ablation and plasma: Laser induced breakdown spectroscopy signal enhancement," Spectrochimica Acta Part B-Atomic Spectrosc. **61**, 999 (2006).
5. Celio Pasquini; Juliana Cortez; Lucas M. C. Silva; Fabiano B. Gonzaga "Laser Induced Breakdown Spectroscopy, J. Braz. Chem. Soc. 18(3), 463 (2007).

Task 3

High Efficiency Particulate Air (HEPA)

Rangaswami Arunkumar and Charles A. Waggoner

INTRODUCTION

The HEPA Filter Performance Assurance task provides data needed to address issues relating to the performance of high efficiency particulate air (HEPA) filters. Both the Defense Nuclear Facilities Safety Board (DNFSB) and state regulators have questioned to what degree DOE can rely on the performance of HEPA filters to satisfy safety and regulatory controls in DOE facilities. A National Technical Working Group was established among DOE, the EPA, interested states, and ICET to develop a plan to resolve these issues. This plan has been accepted by all parties, and has withstood two ASME peer reviews. The latter endorsed the need for the program, "Based on its technical merit, the HEPA Filtration Monitoring project should be continued... The successful completion of this project has broad implications for all applications where ultra-low particulate matter emissions are important. The need for these experimental data is unquestionable." This year the focus is on evaluating the performance of HEPA filters under severe conditions including: increased velocities, temperature extremes, elevated relative humidity, increased mass loadings, wet aerosols, and smoke. The results are anticipated to allow for the establishment of operating envelopes based upon the data and associated safety factors that will provide a more realistic expectation for use of these critical units.

WORK ACCOMPLISHED

A number of activities and accomplishments can be reported for the second quarter of 2008. Active participation and contributions were made during the spring meeting of the ASME Committee on Nuclear Air and Gas Treatment in April. This included presentations to both the Filtration Subcommittee and the Section FI working group. Additional input in the development of Section FI was provided in three conference calls of the working group along with a small group meeting scheduled to correspond with a visit to SRNL. Substantive progress has been made over the past six months and an ICET representative will present an update on the status of Section FI at the Nuclear Air Cleaning Conference in late August. Abstracts for two more papers describing work done at ICET were accepted for the same conference.

Initial development of procedures has been conducted to autopsy the HEPA filters that have been accumulated over the past three years of testing at ICET. These procedures allow the systematic examination of filters that have been loaded with highly characterized aerosols under known conditions to demonstrate the effects of particle size distributions and media velocity on loading patterns within filters. Very little descriptive information of this nature is found in the open literature and evaluation of filters used in previous studies will provide maximum value for the investment of time and materials in previous studies. Additionally, information generated from filter autopsies will provide definitive evidence of effects of media velocity to resolve questions associated with changing the 5 feet per minute maximum currently allowed by the AG-1 standard. Figure 6 shows a filter originally loaded with 434 g of KCl in 2003 that was chosen for autopsy. The plot shows the loading curve for this filter, mass gained as a function of increased differential pressure. Figure 7 shows the steps taken in the procedure utilized to deconstruct this filter allowing examination of the filter pack.

A paper submitted to the Journal of Occupational and Environmental Hygiene was reviewed and ICET authors submitted responses to reviewer comments in late April. Notification was received from the journal in late June that the paper had been accepted for publication and will appear in the November issue. The paper is entitled "The Effects of Media Velocity and Particle Size Distribution on Most Penetrating Particle Size and Filter Loading Capacity of 12"x12"x11.5" AG-1 HEPA Filters."

ICET HEPA filter task team members are chairing two sessions at WM09 on filtration, for air and liquid media. Initial efforts have been undertaken during the 2nd quarter to solicit papers for the 09 conference and have similar sessions be included in the future.

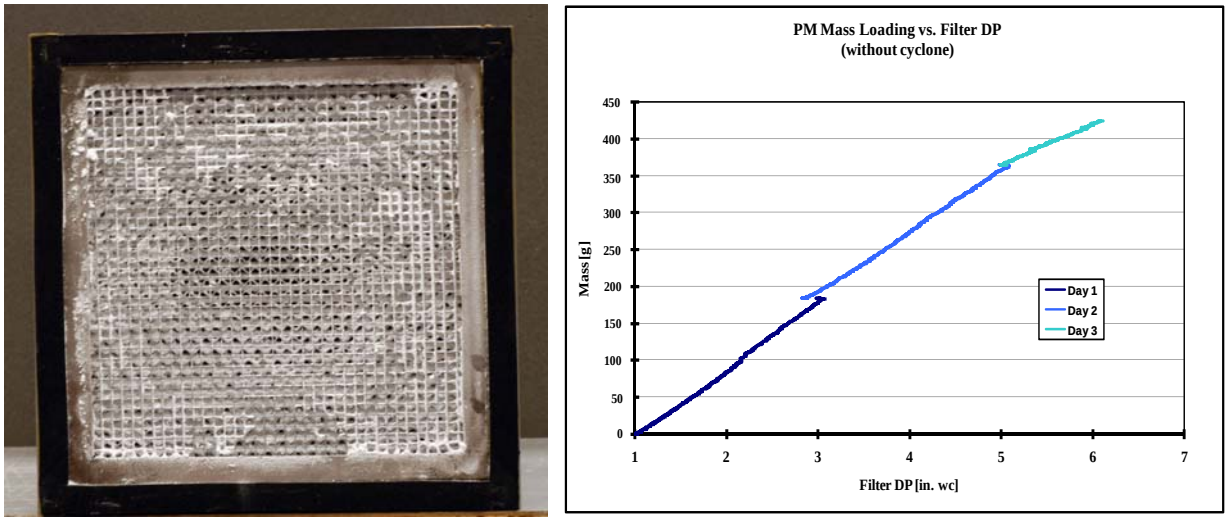

Figure 6. Filter loaded with 434 g KCl in 2003. Left: Face of the loaded filter. Right: Mass loading curve for the filter.

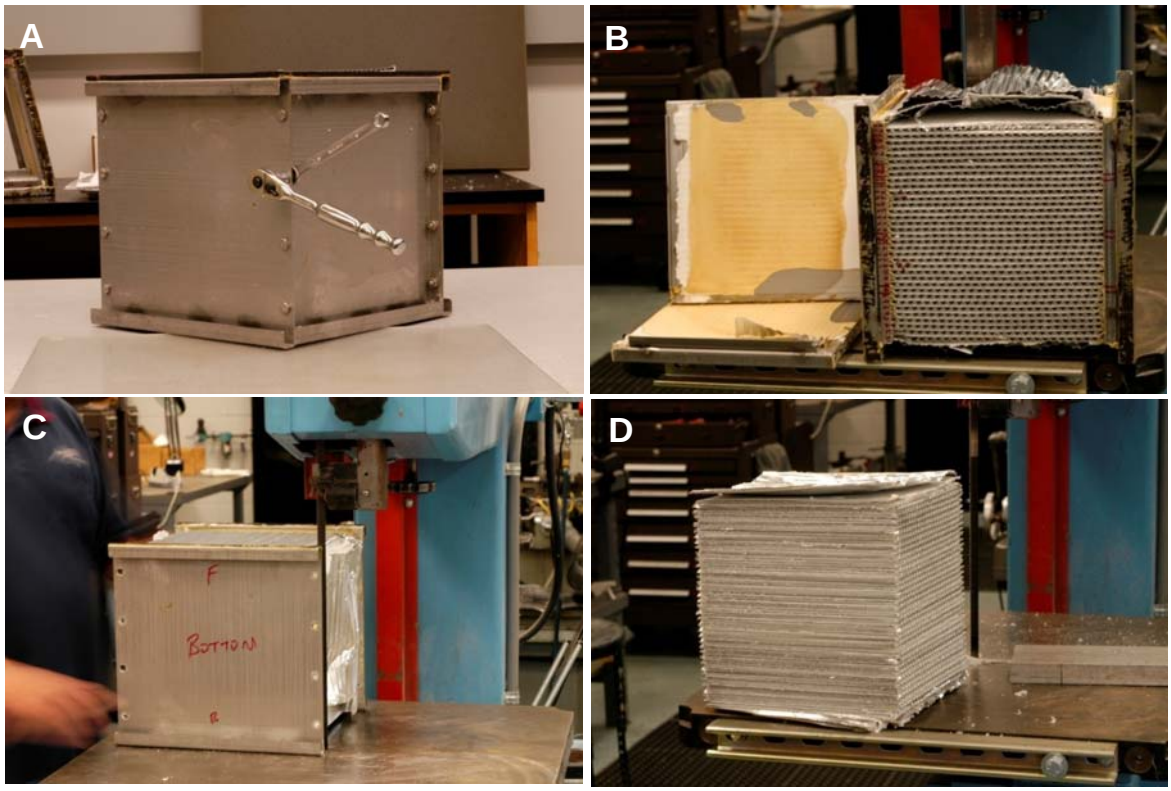

Figure 7. Procedure for deconstruction of filter; i.e., removal of filter pack. A: Removal of bolts from housing. B: Removal of housing ends. C. Removal of top and bottom of housing. D: Filter pack after removal.

WORK FORECAST

Work will continue on the post-performance evaluation of filter media. A number of papers and presentations are in preparation for dissemination of the results obtained to date.

CONCLUSIONS

Work continued on establishing standards for HEPA filter use in nuclear and defense facilities. Procedures for performing autopsies on filter media have been established.

Task 4

Support of Hanford Single Shell Tank Waste Disposition

Jeffrey Lindner, John Luthe, Larry Pearson, Laura Smith, Rebecca Toghiani

INTRODUCTION

Knowledge of the chemistry associated with the wastes contained in the Hanford tank farms has bearings on waste pretreatment, retrieval, vitrification, alternative processing, and tank closure operations. Much of the work conducted at ICET has focused on developing an understanding of the salt chemistry found in these tanks. A number of experiments have been performed and have led to the development of the V7DBLSLT thermodynamic database for use in the OLI Systems Inc. Environmental Simulation Program (ESP). This work consisted of extensive solubility measurements of specific sodium salt systems at the temperatures and pH values typical of the site waste [i,ii]. Additional efforts were directed at aluminum chemistry and with development of a neural network model based on a framework of ESP simulations for use in conjunction with the Hanford H2 (overall campaign flowsheeting) simulator.

The Hanford Tank Waste Operations Simulator (HTWOS) is used for scheduling the entire retrieval campaign and includes model representations for vitrification and low activity waste processes. Chemistry representations used in the (HTWOS) rely on wash and leach factors as opposed to direct, solid-liquid equilibrium thermodynamic calculations. Site engineers have previously requested an evaluation of the feasibility of upgrading the chemistry representation to include ESP. Having a proper chemistry representation within HTWOS will reduce the uncertainties associated with wash and leach factors. Earlier work identified the use of a neural network as a preferred option due to the large number of calculations needed during a HTWOS campaign run. As an initial evaluation of this approach, site engineers requested the application of the process to the retrieval of C farm tanks.

The development of a neural network for use within the HTWOS model requires an extensive set of training data. To generate this data, ICET constructed an ESP program process model of the retrieval of C tank waste based on the procedures and constraints followed in the Modified Sluicing Method [iii] of waste retrieval. With this ESP simulation framework, a neural network training set consisting of the input stream values and the ESP computation output can be built. Construction of the training set to cover the ranges of possible input streams requires an execution of the ESP program for each case. Since ESP is an interactive program, a batch mode processing routine is necessary to replace the ESP user interface. Perl [iv], a freely available platform independent programming language was used to provide this batch mode processing. The retrieval of C-108 waste using flush liquid from AN-106 was simulated with the ESP

program process model and Perl to provide the initial neural net training data. Simulations of each of the remaining C farm tanks, using this model, will provide the data necessary for the generation of an expanded neural network training set applicable across the entire range of C farm tank compositions. This expanded neural network will allow an evaluation of the retrieval schedule including different combinations of source and destination tanks. Since the neural network utilizes equilibrium chemistry as its basis, the potential result is a more accurate, as well as, timely method for Hanford campaign simulation.

WORK ACCOMPLISHED

The retrieval of waste from the Hanford C farm tanks is currently scheduled to utilize two waste recovery techniques. The Modified Sluicing with Recycle method (MSwR) has been selected for use in the majority of tanks. This method has been modeled using the OLI ESP equilibrium program as reported previously [1,2]. The second technique to be used in the C farm area is the Mobile Retrieval System (MRS).

Modeling of this retrieval method was performed utilizing the OLI ESP equilibrium program to be consistent with the prior MSwR simulations. The basic structure of the MSwR model was maintained as shown in Figure 8. The simulation was modeled based on data obtained from Hanford regarding the procedures and constraints followed in the Mobile Retrieval System of waste retrieval. This retrieval method consists of 2 stages which are defined based on 1) the amount of waste remaining in the tank and 2) the percent of entrained solids attained. Table 7 describes the stages as they were modeled.

Table 7 - Mobile Retrieval System Stages

Stage	Ending tank waste volume (gal)	Retrieved waste volume (gal)	Solids entrainment (vol%)
1	30,000		22.0
2	2,693		2.0

In addition to the individual stage conditions, certain constraints were used for the total retrieval process as follows:

1) 1,200 gallons of waste were retrieved per day.
2) Maximum specific gravity of any processed stream of 1.3.
3) Maximum Na concentration of any processed stream of 5.0 gmoles/liter.

The retrieval of waste from C-101 into AY-101 was chosen to model as it is the first MRS retrieval scheduled under the C farm overall plan shown in Table 9. Although the schedule shows the MSwR retrieval of C-107 into AY-101 prior to the MRS recovery of C-101, it was

decided to develop the MRS model using the initial AY-101 composition. Once the model has been developed, the simulations will be rerun according to the C farm schedule.

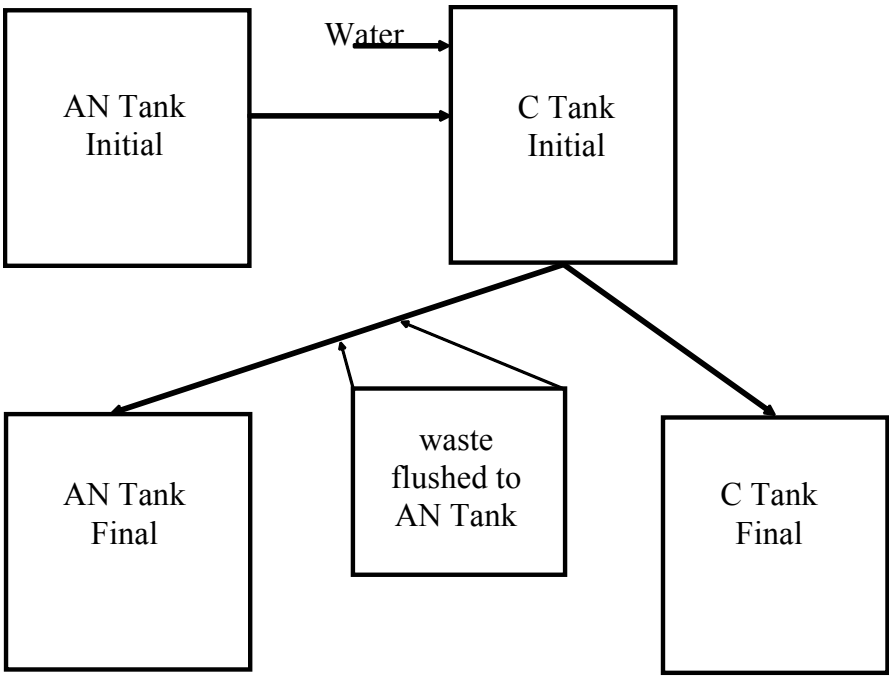

Figure 8 – ESP Model Block Flow Diagram

Table 8 – Hanford C farm Tank Retrieval Schedule

Source Tank	Receiver Tank	Technology
C-108	AN-106	MSwR
C-109	AN-106	MSwR
C-104	AN-101	MSwR
C-107	AY-101	MSwR
C-110	AN-106	MSwR
C-112	AN-101	MSwR
C-101	AY-101	MRS
C-105	AY-101	MRS
C-102	AZ-101	MSwR
C-111	AN-101	MRS

The retrieval of waste from C-101 into AY-101 was simulated using the ESP program and the conditions and constraints listed above. Discussions with Hanford personnel have indicated that, unlike waste retrieval using MSwR, the current plan for MRS is to use only fresh water during waste retrieival. Therefore, it was decided to simulate two cases for comparison. The first case

was the retrieval of C-101 into AY-101 using only fresh water for flushing. The second case was the retrieval using no fresh water for flushing. In this case AY-101 liquid was used for flushing. Table 10 is a summary of the Case 1 simulation. Figures 9, 10, and 11 present additional information.

Table 9 – Case 1 Summary (C-101 to AY-101 with fresh water flush)

	AY-101			C-101		
	Initial	Stage 1	Stage 2	Initial	Stage 1	Stage 2
total volume (gals)	831,484	881,572	1,395,843	47,878	30,121	2,645
wt% water	74.80	74.33	80.86	20.22	19.24	19.63
wt% solids	8.26	8.37	6.76	60.26	73.82	80.02
vol% solids	3.73	3.81	2.91	48.75	59.96	60.84
SpG	1.21	1.21	1.15	1.84	1.85	1.98
Na molarity	3.12	3.22	2.20	5.28	4.18	0.27
pH	12.20	12.20	11.93	13.80	13.19	12.07
ionic strength	3.63333	3.73268	2.59804	12.2378	4.47187	0.401831

AY-101			
Initial	Stage 1	Stage 2	aqueous ion concentration
3.128713	3.208723	2.202729	Na(+1) (m/L)
0.050317	0.057238	0.055236	P(+5) (m/L)
0.329832	0.330218	0.208577	N(+3) (m/L)
1.039604	1.102804	0.709552	N(+5) (m/L)
0.000050	0.000050	0.000027	Fe(+3) (m/L)
0.056780	0.056765	0.036041	acetate (m/L)
0.040295	0.039015	0.061264	oxalate (m/L)

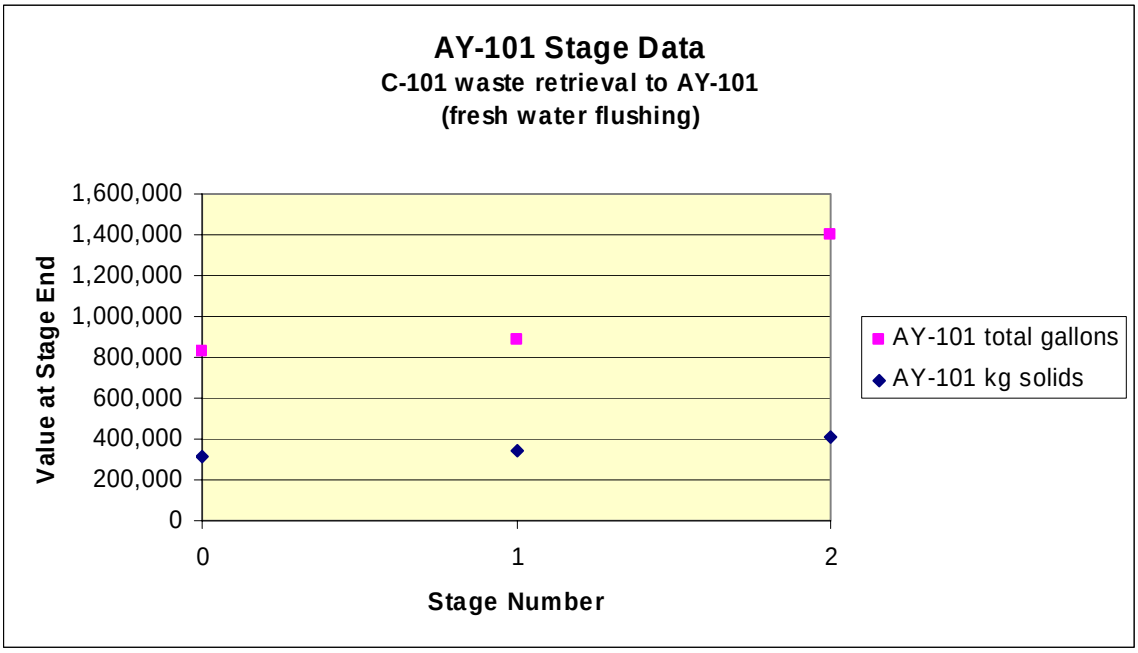

Figure 9 – Case 1 Simulation (C-101 waste retrieval to AY-101)

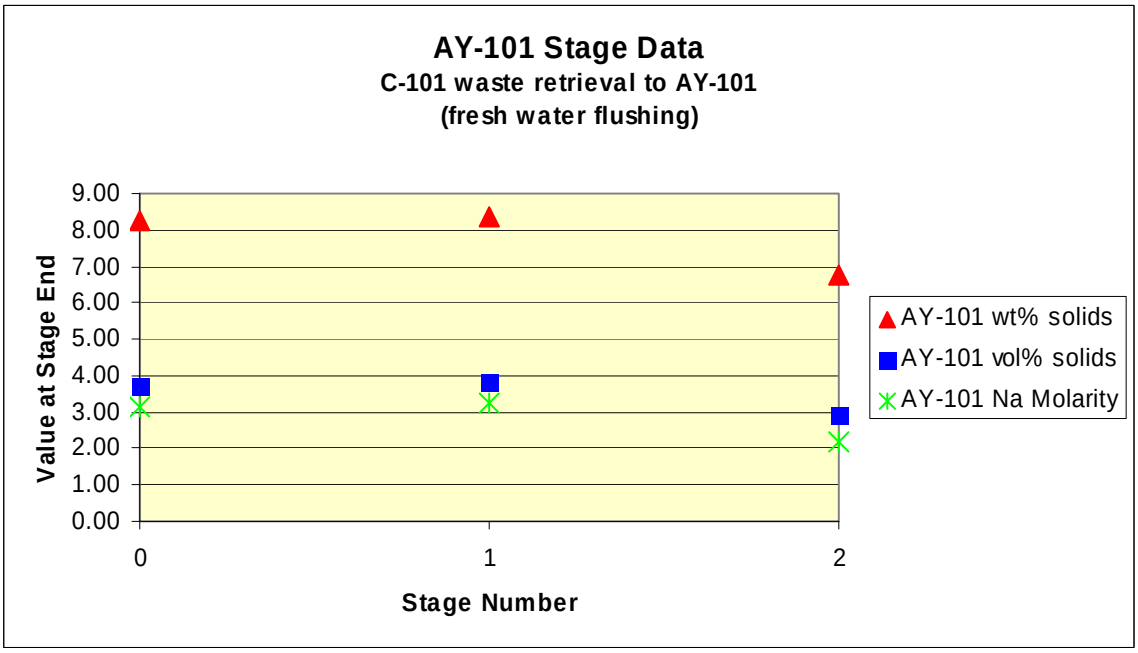

Figure 10 – Case 1 Simulation (C-101 waste retrieval to AY-101)

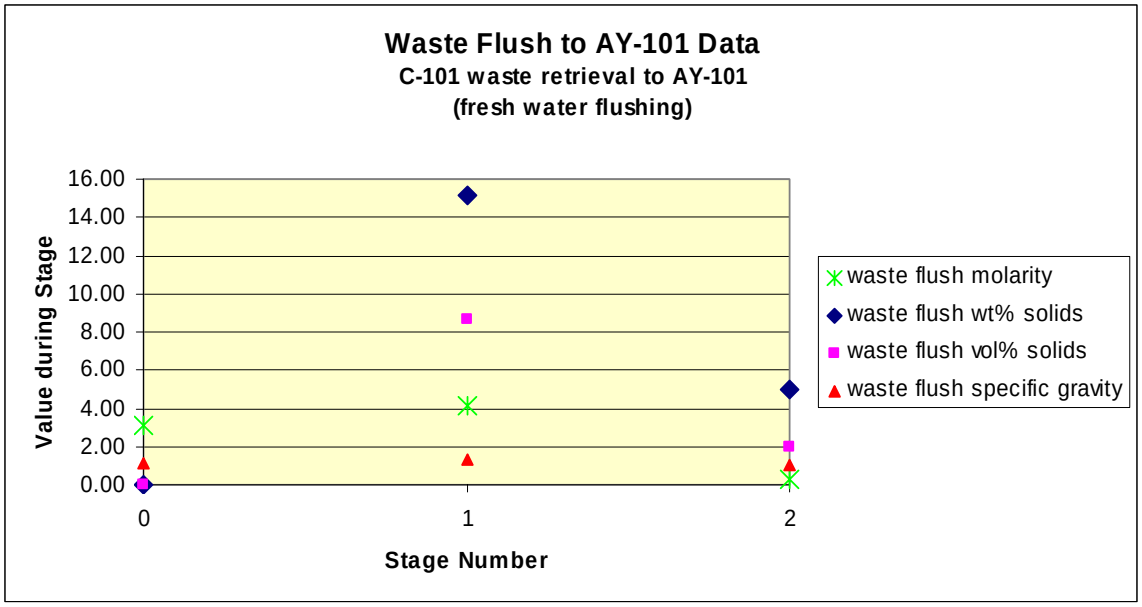

Figure 11 – Case 1 Simulation (C-101 waste retrieval to AY-101)

The Case 1 data shows that the use of only fresh water for flushing results in a significant increase in the waste volume in AY-101. Approximately 525,000 gallons of water is required for the retrieval under the constraints listed above. In addition, the 1.3 specific gravity constraint on transfer streams limited the attained flush solids content (% volume) to well below the 22% target.

Table 10 is a summary of the Case 2 simulation in which AY-101 liquid was used for flushing of C-101 (ie. no fresh water was used). Figures 7, 8, and 9 present additional information.

Table 10 – Case 2 Summary (C-101 waste retrieval to AY-101 with no fresh water flush)

	AY-101			C-101		
	Initial	Stage 1	Stage 2	Initial	Stage 1	Stage 2
total volume (gals)	831,878	848,380	875,617	47,878	30,287	2,717
wt% water	74.96	73.32	71.43	20.23	22.56	17.44
wt% solids	8.26	8.87	10.79	60.26	69.34	78.21
vol% solids	3.73	4.07	5.05	48.75	54.51	62.80
SpG	1.21	1.22	1.24	1.84	1.81	1.99
Na molarity	3.13	3.35	3.44	8.97	4.50	3.44
pH	12.20	12.22	12.22	13.80	13.05	12.38
ionic strength	3.63333	3.88926	4.06591	12.2378	5.17309	4.0821

AY-101			
Initial	Stage 1	Stage 2	aqueous ion concentration
3.126515	3.345916	3.438626	Na(+1) (m/L)
0.050292	0.062152	0.087109	P(+5) (m/L)
0.329670	0.341482	0.340977	N(+3) (m/L)
1.039898	1.149463	1.155680	N(+5) (m/L)
0.000050	0.000052	0.000052	Fe(+3) (m/L)
0.056752	0.058769	0.058680	acetate (m/L)
0.040276	0.037305	0.036584	oxalate (m/L)

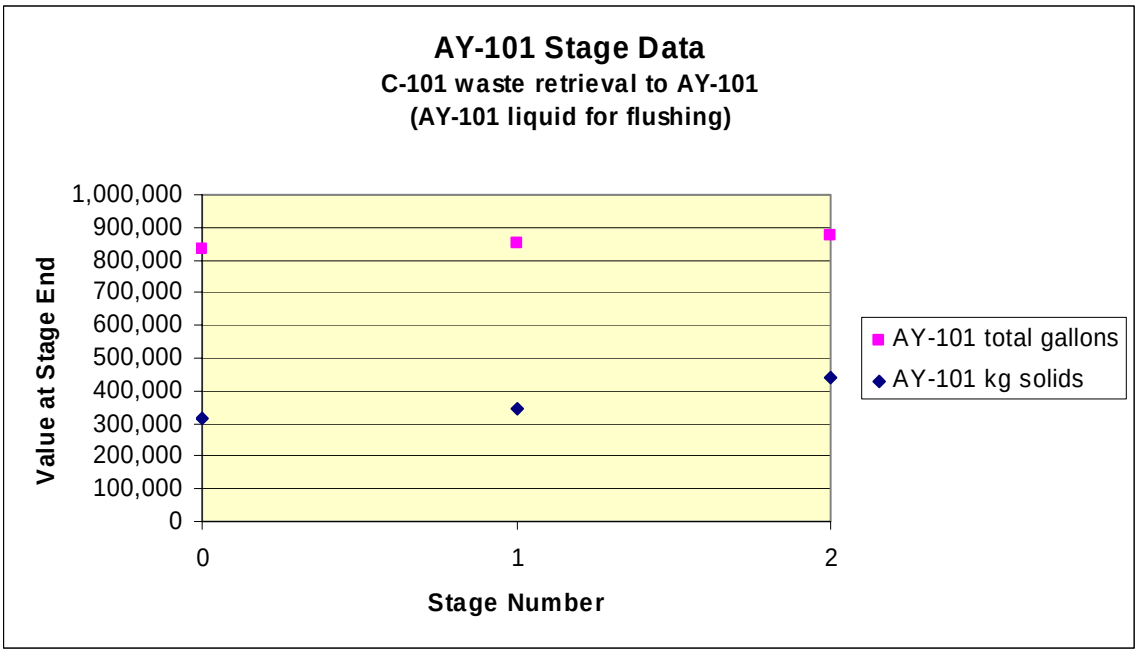

Figure 12 – Case 2 Simulation (C-101 waste retrieval to AY-101)

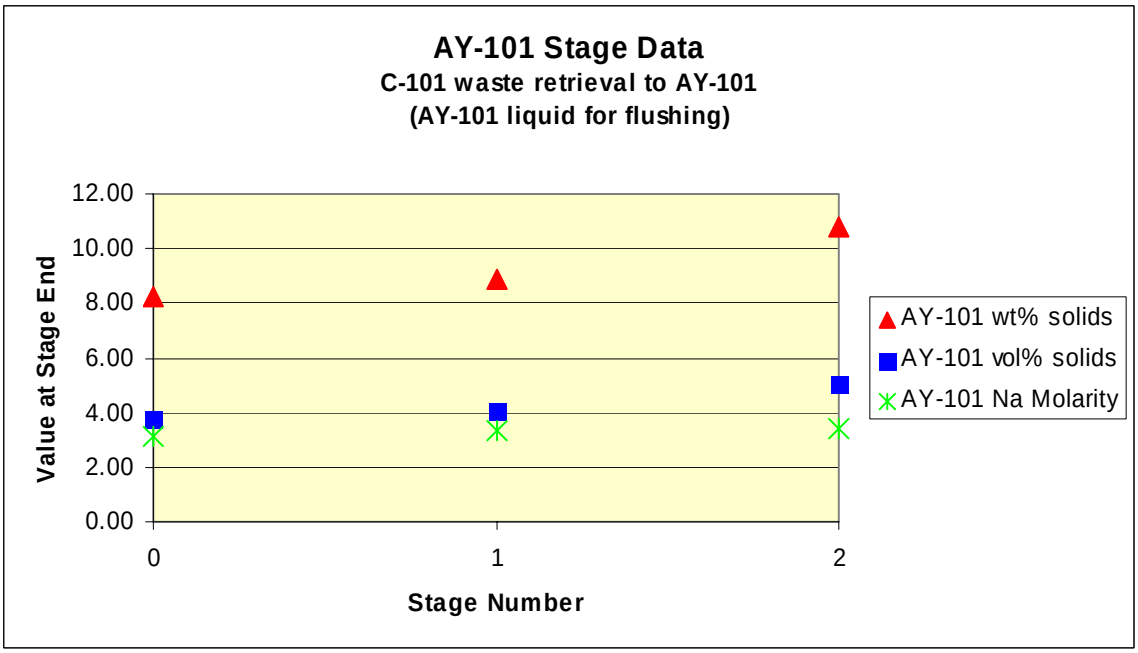

Figure 13 – Case 2 Simulation (C-101 waste retrieval to AY-101)

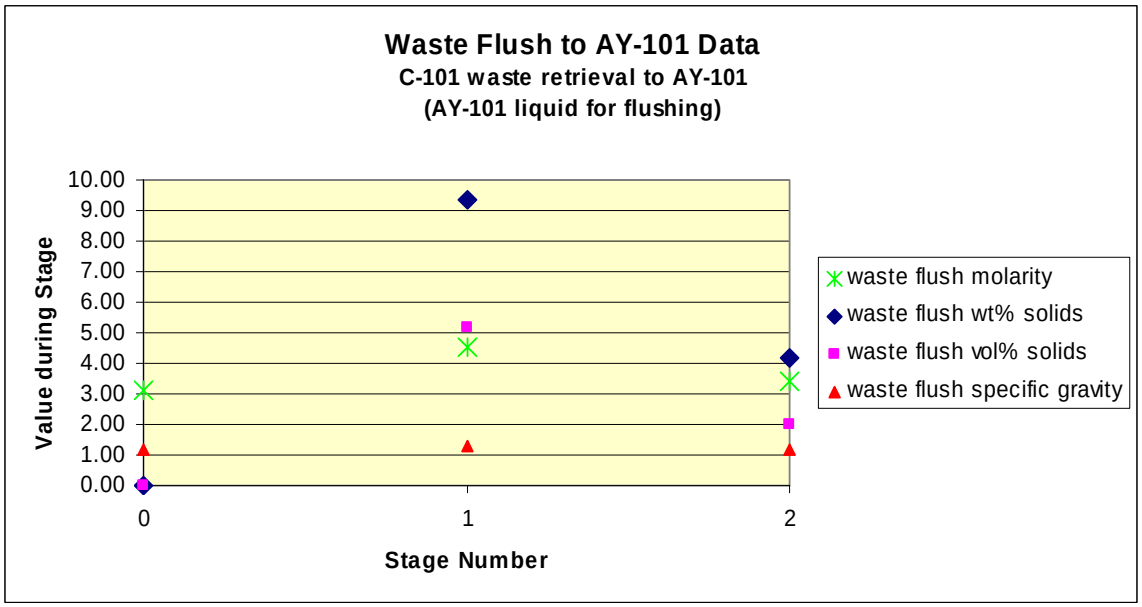

Figure 14 – Case 2 Simulation (C-101 waste retrieval to AY-101)

The Case 2 data shows that the MRS retrieval of C-101 waste into AY-101 can be accomplished using AY-101 liquid for flushing and while meeting all constraints. As compared to the Case 1 use of fresh water for flushing, the final volume of AY-101 is reduced by a significant amount (525,000 gallons). As seen in Case 1, the Case 2 data also shows that the 1.3 specific gravity constraint limits the attainable flush solids (% volume) to well below the target of 22%.

The assembly of a neural network training set to be used for training a neural network description of the C-tank retrieval process continued. The ESP simulation framework for the retrieval of tanks C-108, C-109, and C-110 into AN-101, using the Modified Sluicing Method [5] was used to add to the C-tank neural network training set. The training set contained the stage input stream values for the three C-tank retrieval into AN-106, with the corresponding ESP computation results. This was a test of the batch scripting of the ESP program. The resulting training set, while containing several thousand points, covered a very narrow region of the constituent compound range. The training set was built by varying the AN-106 flush and fresh water flush volumes.

To build a training set that covers the ranges of possible input streams requires an execution of the ESP program for each case. The normal use of the ESP program is as an interactive program, however it is possible to write programs to replace the ESP user input program and execute the ESP computation program in a non-interactive batch mode. The first version of a batch mode processing program, written in Perl [4] (a freely available, platform independent programming language) is limited to a single tank retrieval simulation. Development was begun on a ESP batch mode processing script that can process staged multiple tank retrievals. Such a script is necessary to generate a wider range of ESP input and output cases. The additional data to cover a wider range of possible tank constituent combinations for the training set will be generated by varying the order of tank retrieval as well as the flush rates and solids entrainment.

WORK FORECAST

Additional ESP process simulations will be developed for the other C tank retrievals. In particular, the ESP simulation model will be used to evaluate C tank retrievals using both the modified sluicing (MSwR) and the mobile retrieval system (MRS) methods [6] as per the current Hanford retrieval schedule. Neural network training set data will be generated using the expanded ESP process simulations. Additional batch scripting modules for the ESP program will be developed for stages of the process simulations, as needed to build the neural network training sets.

CONCLUSIONS

An ESP process simulation model, which approximates the C tank farm Mobile Retrieval System for waste retrieval has been used to evaluate the retrieval of C-101 waste into AY-101. In addition, a comparison of the use of fresh water versus AY-101 liquid for flushing was accomplished. The results of the comparison showed that AY-101 liquid could be used instead of fresh water for flushing while maintaining all modeling constraints. If fresh water is eliminated from the MRS method (for this C-101 to AY-101 scenario) approximately 500,000 gallons of AY-101 tank volume are saved. This ESP process model will be used to generate data to train a neural network representation of the C tank farm retrieval chemistry for use in HTWOS. Batch mode processing programs for ESP have been tested to generate single tank retrieval data for the neural network training set. Development has begun extending the programs to sequential multiple tank retrievals.

REFERENCES

1. Toghiani, R. K., Phillips, V. A., and Lindner, J. S., "Solubility of Na-F-SO_4 in Water and in Sodium Hydroxide Solutions," Journal of Chemical and Engineering Data 50(5), 1615, (2005).

2. Selvaraj, D. K., (2003), Solubility Studies in the Na-F-PO_4 System in Sodium Nitrate and in Sodium Hydroxide Solutions, MS Thesis, Chemical Engineering, Mississippi State University, Mississippi State, MS.

3. Lindner, J.S., Luthe, J.C., Pearson, L.E., Smith, L.T., Toghiani, R.K., (2007), "Process Chemistry and Operations Planning for Hanford Waste Alternatives" in "Accelerating Cleanup of the Defense Nuclear Legacy," ICET Quarterly Technical Progress Report for the period July 1, - September 31, 2007, Report Number 07040R03 U. S. Department of Energy Agreement Number DE-FC01-06EW-07040, Mississippi State, MS.

4. Larry Wall, Tom Christiansen, Jon Orwant, "Programming Perl," Third Edition, O'Reilly, Sebastopol, CA 2000.

5. Lindner, J.S., Luthe, J.C., Pearson, L.E., Smith, L.T., Toghiani, R.K., (2008), "Process Chemistry and Operations Planning for Hanford Waste Alternatives" in "Accelerating Cleanup of the Defense Nuclear Legacy," ICET Quarterly Technical Progress Report for the period January 1, - March 31, 2008, Report Number 07040R05 U. S. Department of Energy Agreement Number DE-FC01-06EW-07040, Mississippi State, MS

6. R.A. Dodd, J.W. Cammann, "Progress in Retrieval and Closure of First High-Level Waste Tank at Hanford: Single-Shell Tank C-106," WM'05 Conference, February, 2005, Tucson AZ.

Task 5

Phytoremediation and Long-Term Monitoring of Heavy Metal Contaminants

Yi Su, Fengxiang Han, and David Monts

INTRODUCTION

To date, no natural plant species has been reported as hyperaccumulator for mercury phytoremediation. Indian mustard, a high biomass plant with faster growth rates has showed potential for heavy metal phytoremediation. However, the toxicology (biomass, leaf water content, and leaf structure) impacts of Hg on Indian mustard have not been studied.

WORK ACCOMPLISHED

A greenhouse experiment on effects of Mg level on Hg uptake, accumulation and toxicology by two varieties of Indian mustard was conducted.

Meanwhile, analyses on previous greenhouse studies on oxidative stress of Indian mustard by Hg in terms of leaf structure change and biomass effects were continued. Mercury showed a significant phytotoxicity in two cultivars of Indian mustard at elevated solution Hg concentrations ($\geq$2 mg L^{-1}). Phytotoxicity of ionic mercury to Indian mustard resulted in the reduction of biomass and relative water contents of both shoots and roots in these two cultivars (Figs. 10 and 11). Biomass of both shoots and roots followed a logarithmic decrease with mercury concentrations in both shoots and roots. Initially, biomass of both shoots and roots quickly decreased with mercury concentration in plants, followed by a very slow change at higher mercury concentration (Fig. 15). The critical mercury concentrations in roots causing 25% or 50% decrease in biomass were significantly higher (20-30 times) than those in shoots. Moreover, these critical mercury concentrations in both shoots and roots increased with the age of plants. Mature Indian mustard plants (30/45-day-old) had significantly higher critical mercury concentrations in both shoots and roots than younger plants (15/23 day-old). Mercury concentrations in younger plants (15/23-day-old) causing 25% biomass decrease in shoots and roots were 30 and 740 mg/kg, respectively. But the critical mercury concentrations in the mature plants (30/45-day-old) causing 25% reduction of biomass in shoots and roots increased to 168 and 3250 mg/kg, respectively. Similar trends were observed for the critical mercury concentrations in plants causing 50% biomass decreases. This indicates that the two cultivars of Indian mustard significantly increased their tolerance to mercury and the amount of mercury

translocated to shoots with age. Another important indicator of mercury toxicity is relative water contents (RWC). RWC (%) of shoots significantly decreased with mercury concentrations in plants (Fig. 16).

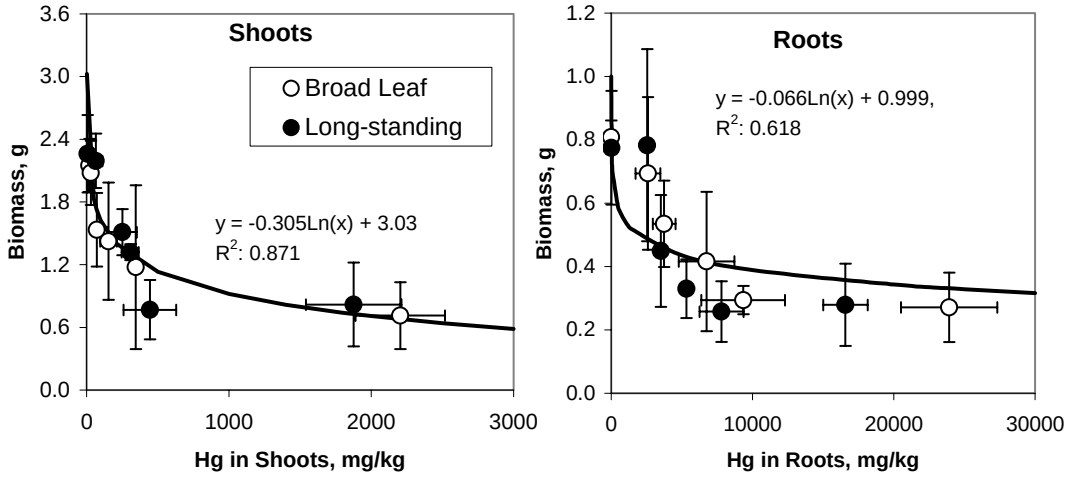

Fig. 15. Effect of mercury on biomass production (as average and standard deviation for each treatment level) of the two cultivars of Indian mustard (1-month-old plants after 2 weeks of mercury treatment). There were no significant differences between the two cultivars and a fast decrease in biomass to about 25% at higher mercury concentrations.

Microscopic study indicated that elevated mercury concentrations in plants significantly changed leaf cellular structure: thickly stained areas surrounding the vascular bundles, decreases in the number of palisade and spongy parenchyma cells, reduced cell size and clotted depositions, and decreases in size and number of vacuoles along the cell walls. The palisade chloroplasts exhibited decreases in their amounts and starch grains as well as a loss of spindle shape (Fig. 12).

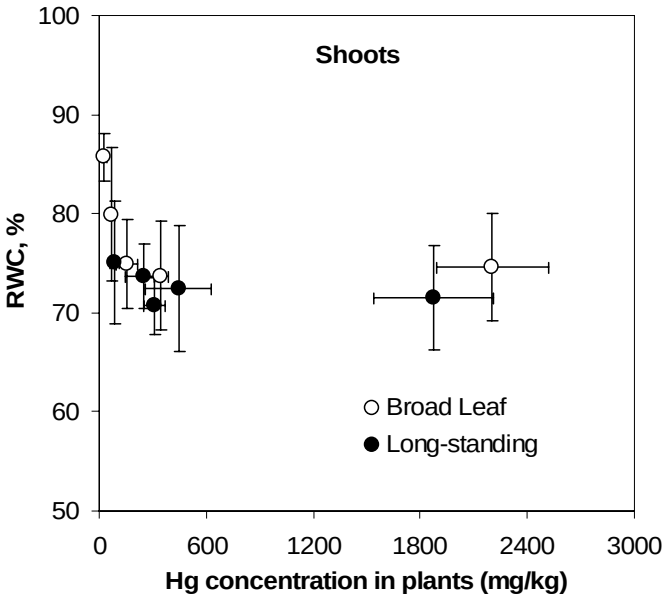

Fig. 16. Effect of mercury on leaf relative water content (%) of the two cultivars of Indian mustard (1-month-old plants after 2 weeks of mercury treatment). The relative water contents in shoots initially significantly decreased with mercury concentrations in shoots from about 90% to 70%, followed by a slow change with further increases in mercury concentration.

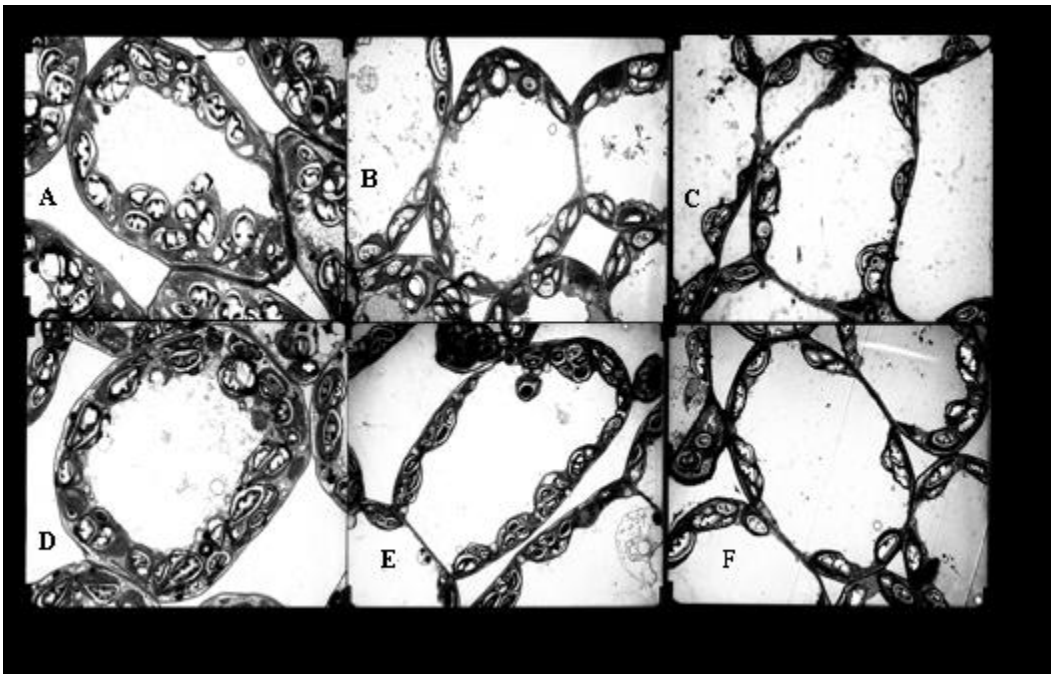

Fig. 17. TEM micrographs showing decreases in chloroplasts and starch grains of lower palisade parenchyma leaf cells of Hg-treated plants (1-month-old) of cultivar Broad Leaf and Long-standing after 2 weeks exposure to mercury solution (A, B, and C were the

control, 4.11, and 16.7 mg L^{-1} mercury treatments for the cultivar Broad Leaf, respectively; D, E, and F the control, 4.11, and 16.6 mg L^{-1} mercury treatments for the cultivar Long-standing, respectively).

Chemical analysis showed high accumulation of mercury in plant tissues, especially in roots. This result indicates Indian mustard might be a potential candidate plant for phytofiltration of contaminated water and phytostabilization of mercury contaminated soils.

CONCLUSIONS

Based on high accumulation of mercury in plant tissues, especially in roots, and defensive oxidative response of Indian mustard to Hg, Indian mustard might be a potential candidate plant for phytofiltration / phytostabilization of mercury contaminated waters and phytostabilization of mercury contaminated soils. More experiments are planned to verify these findings.

WORK PLANNED FOR NEXT QUARTER

Continue greenhouse studies on the effects of Hg on physiological status of selected plant species.

Task 6

SRS Saltstone Process Studies

Ronald Palmer, R. Arunkumar and Walter Okhuysen

INTRODUCTION

This project is comprised of two subtasks. The first consists of laboratory scale experiments designed to examine the thermal properties of new saltstone formulations. The second consists of Pilot Scale studies.

Laboratory Scale Experiments

Small batches prepared in the laboratory must be done prior to designing the pilot scale tests. Lab methods will be set up for measuring the heat of hydration for various saltstone formulations.

Mixers capable of providing batches from as small as several 10s of grams to more than one kilogram are available in the ICET laboratory. A standard protocol for making these small batches will be developed.

An adiabatic calorimeter will designed and built to measure the heat of hydration of the saltstone formulations. This device will provide basic thermal property measurements. These data are important contributions to new revisions of the Performance Assessment documentation.

Pilot Scale Studies

Small batches prepared in the laboratory can only provide preliminary information. A pilot-scale facility, capable of producing 55-gallon drum sized product, is available at the ICET laboratories. Drums can be appropriately instrumented to examine the heat generation of Saltstone formulations on an intermediate scale between the laboratory and actual Saltstone production facility.

Using these same waste simulant recipes, various formulations of saltstone will be produced at our pilot-scale facility. The laboratory scale work provides the basis for determining which formulations to study further. The results of this work will provide the confidence necessary for full scale production at the saltstone production facility.

WORK ACCOMPLISHED

Discussions were held with representatives of Savannah River regarding the scope of this project. The following activities have been defined for the laboratory scale experiments:

- Establish protocol for making salt solutions and small batches of saltstone formulations
- Design and build an adiabatic calorimeter
- Set up to measure heat of hydration using the adiabatic calorimeter
- Design experiments with 1kg batches studying the heat evolution of the Saltstone formulations using containers outfitted with thermocouples

The following activities have been defined for the pilot scale experiments:

- Design thermocouple system for measuring thermal behavior in pilot scale system
- Measure heat generated in mixing tank and receiving drum
- Test pilot-scale system with reference saltstone
- Test pilot-scale system with new saltstone formulation(s)

WORK FORECAST

The following tasks are expected to be active during the next quarter:

- Establish protocol for making salt solutions and small batches of saltstone formulations
- Design and build an adiabatic calorimeter
- Design thermocouple system for measuring thermal behavior in pilot scale system

REFERENCES

1. Steimke, J. L. and M. D. Fowley, "Measurement of Thermal Properties of Saltstone," WSRC TR-97-00357, Westinghouse Savannah River Company, Aiken, SC, 1997.
2. Harbour, J. R. et al., "Characterization of Slag, Fly Ash and Portland Cement for Saltstone," WSRC-TR-2006-00067, Revision 0, Savannah River National Laboratory, Aiken, SC, 2006.
3. Harbour, J. R. et al., "Heat of Hydration of Saltstone Mixes – Measurement by Isothermal Calorimetry," WSRC-STI-2007-00263, Revision 0, Savannah River National Laboratory, Aiken, SC, 2007

Task 7

Bioavailability Studies of Mercury and other Heavy Metal Contaminants in Ecosystems of Selected DOE Sights

Fengxiang X. Han, Yi Su, David L. Monts, and Charles A. Waggoner

INTRODUCTION

Many subsurface minerals may modify the stability of HgS and release trace amount of mercury from contaminated subsurface. Two common Fe oxides (magnetite, Fe_3O_4; hematite, Fe_2O_3) are common minerals found in the subsurface of Oak Ridge site. The oxidation rates of HgS by Fe oxides may be expressed by release of SO_4 into soil solution.

WORK ACCOMPLISHED

The previous laboratory simulation studies showed magnetite with high oxidation potential significantly oxidized HgS from contaminated Oak Ridge soil, release increased SO_4, while hematite released very little amount of SO_4, indicating hematite had a limited effect on stability of HgS in soil and subsurface of Oak Ridge site.

CONCLUSIONS

Further studies are needed to draw conclusion.

WORK PLANNED FOR NEXT QUARTER

With the coming of the ICET funding, this project was resumed to its full scale.

IN-TANK CHARACTERIZATION FOR CLOSURE OF HANFORD WASTE TANKS

David L. Monts

INTRODUCTION

The goal of this project is to develop and deploy in-tank waste characterization tools for use at the Hanford Site. These will be used to reduce uncertainties and risks associated with waste processing and closure activities. Some of the systems developed for this effort are also applicable to other DOE sites, such as the Savannah River Site.

After as much waste as practical has been removed from the tank, analyses of remaining deposits will be needed to determine the long-term risk associated with the residual waste and to determine the appropriate steps required for closure. These needs are described in Hanford Technical Challenges WT-115, Technology to Support Post-Retrieval Evaluation of SSTs and also in DOE-EM Engineering & Technology Roadmap, Improve Residual Waste Tank Characterization and Stabilization.

ICET will assemble and test the following systems for potential deployment for nondestructive, *in situ* imaging means of quantitatively determining the volume and height of waste (including that deposited on tank walls, and the volume and depth of sediments), based on Fourier-transform profilometry (FTP) and stereovision (SV). FTP images are obtained by using a white light source to project a fringe pattern onto the object of interest and using a camera to record the resulting distortions of the fringe pattern due to reflection from non-flat surfaces. A software package has been developed by ICET that automatically processes the FTP image to yield quantitative measurements and renderings of the object. In some cases, tank solids are covered by a layer of pipeline flush water, following the completion of retrieval. Quantitative mapping of tank sediments would enable a more accurate determination of the volume of residual tank wastes. Sediment mapping is not feasible with currently deployed instrumentation. FTP will evaluate the feasibility of sediment mapping under a variety of conditions. Stereovision also provides 3-D topographical reconstruction of target surfaces by using images simultaneously recorded by two or more cameras from different viewpoints.

During CA07, ICET's efforts for this task are to include:

- During CA06, the Fourier transform profilometry (FTP) probe effort initiated a series of FTP performance evaluation tests under simulated Hanford waste tank conditions. The purpose of these tests is to test and document the accuracy, precision, and operational performance using blind testing techniques. Nondescript targets have been created and their volumes determined by traditional methods, but the values of the volumes were not known to those ICET personnel who used FTP to quantitatively determine their volumes. The first stage of this testing involved simulating objects on the bottom of a flat C200-series Hanford waste tank and analyzing the volume of individual objects from single FTP images. The second stage involves using new non-descript targets and determining the total volume present by "stitching" the results of individual images together. These tests will demonstrate the performance of the FTP system prior to demonstration in Hanford's Cold Test Facility (CTF). In order to test the durability and reliability of components comprising the FTP system, a series of tests have begun subjecting selected components to gamma-ray radiation. All FTP tests are being conducted with frequent consultation with our Hanford collaborators.

- The Stereovision effort has developed and improved the ICET Stereovision system with better cameras, and has also evaluated a variety of algorithms for stereomatching. Our results show that performance (accuracy and computer analysis time) of a stereomatching algorithm often varied with specific test images. The stereovision system and algorithms have been tested with images of selected targets at different working distances. For Hanford tank inspection, parallel implementation of stereomatching algorithms is necessary because large image size and disparity search range are inevitable.

WORK ACCOMPLISHED:

At the end of March, ICET was informed that because of the downward revision of the ICET Cooperative Agreement CA08 budget, that there are no funds to support the Hanford in-tank characterization effort for the current Cooperative Agreement year. ICET administrators subsequently issued a stop-work order. The bi-weekly conference calls with our Hanford collaborators were suspended. At this time, no further efforts are planned until funding becomes available. Efforts have begun to seek funding for the FTP technical feasibility report requested by our Hanford collaborators.

WORK PLANNED

When funds become available, work on this effort will resume. The FTP technical feasibility study and report requested by our Hanford collaborators will be our first priority when funding is available.

ACRONYMNS

CTF	Cold Test Facility
FTP	Fourier transform profilometry
ICET	Institute for Clean Energy Technology
SV	stereovision